
3D GAUSSIAN AS A NEW VISION ERA: A SURVEY

A PREPRINT

Ben Fei^{*,1}, Jingyi Xu^{*,1}, Rui Zhang^{*,1}, Qingyuan Zhou^{*,1}, Weidong Yang^{†,1}, Ying He^{†,2}

¹Fudan University, ²Nanyang Technological University
bfei21@m.fudan.edu.cn, wdyang@fudan.edu.cn, yhe@ntu.edu.sg

ABSTRACT

3D Gaussian Splatting (3D-GS) has emerged as a significant advancement in the field of Computer Graphics, offering explicit scene representation and novel view synthesis without the reliance on neural networks, such as Neural Radiance Fields (NeRF). This technique has found diverse applications in areas such as robotics, urban mapping, autonomous navigation, and virtual reality/augmented reality, just name a few. Given the growing popularity and expanding research in 3D Gaussian Splatting, this paper presents a comprehensive survey of relevant papers from the past year. We organize the survey into taxonomies based on characteristics and applications, providing an introduction to the theoretical underpinnings of 3D Gaussian Splatting. Our goal through this survey is to acquaint new researchers with 3D Gaussian Splatting, serve as a valuable reference for seminal works in the field, and inspire future research directions, as discussed in our concluding section.

Keywords 3D Gaussian Splatting, rendering, reconstruction, generation, perception, virtual humans, manipulation, computer graphics.

1 Introduction

3D Gaussian Splatting (3D-GS) has emerged as a prominent technique in the field of computer graphics, particularly in the context of 3D rendering [Kerbl et al., 2023, Lu et al., 2023, Yu et al., 2023a]. 3D-GS offers a versatile and powerful approach for efficiently rendering complex scenes with high levels of detail [Wu et al., 2023a, Cotton and Peyton, 2024]. By representing objects and surfaces as a collection of Gaussians, Gaussian splatting allows for the efficient and accurate representation of geometry and appearance properties [Guédon and Lepetit, 2023, Yu et al., 2023a]. 3D-GS overcomes the limitations of volume rendering methods by providing a more flexible and adaptive representation of 3D objects [Kerbl et al., 2023]. Additionally, Gaussian splatting enables realistic rendering of various visual effects such as depth-of-field and soft shadows, making it a valuable tool in computer graphics research and applications [Chung et al., 2023a].

The main contribution of this paper is to provide a comprehensive overview of 3D Gaussian Splatting, exploring its underlying advancements and applications. Through an extensive review of existing literature, we aim to present a detailed analysis of the techniques and algorithms used in 3D Gaussian splatting, including the mechanisms of Gaussian generation, reconstruction, manipulation, perception, and human applications. In addition to examining the current state-of-the-art in 3D-GS, this paper also aims to highlight the challenges and open research questions in this field. We will delve into topics such as efficient data structures for handling large-scale scenes, optimization techniques for real-time rendering, and the integration of 3D-GS with other rendering algorithms. Furthermore, we will discuss various applications of 3D-GS, ranging from robotics to autonomous navigation. By identifying these research gaps, we hope to inspire future work and foster advancements in the field of 3D Gaussian splatting.

Overall, this comprehensive review will contribute to a deeper understanding of Gaussian splatting and its potential applications in various domains. Our main contributions are listed below.

*Equal contribution, †Corresponding author.

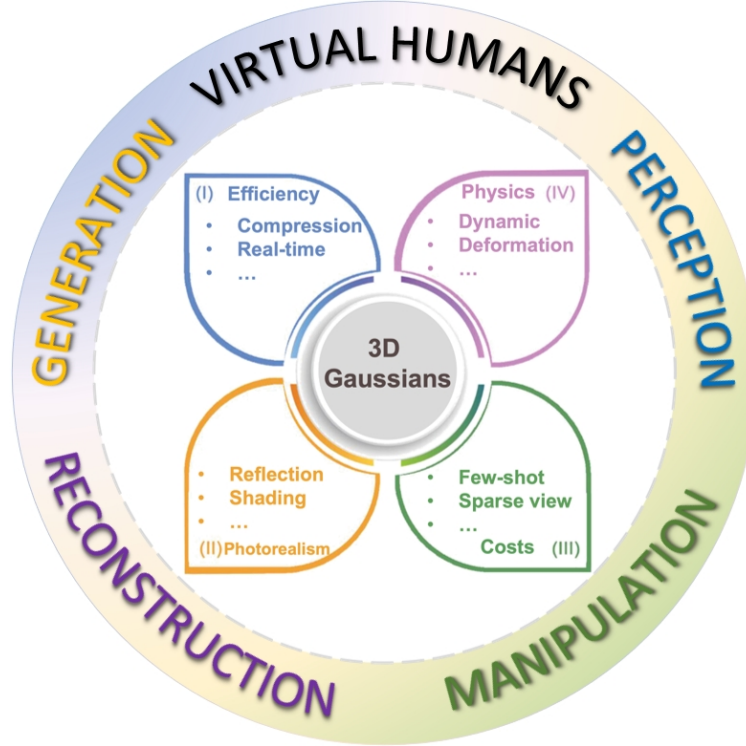


Figure 1: The framework of this survey. The optimization of 3DGS will be first introduced in terms of efficiency, realness, costs, and physics. Then, 3DGS on reconstruction, manipulation, perception, generation, and human applications are comprehensively reviewed.

- **Unified framework with systematic taxonomy.** We introduce a unified & practical framework for categorizing existing works in 3D Gaussians. This framework divides the field into 6 main aspects. Additionally, we provide detailed taxonomies of applications of 3D Gaussians offering a comprehensive perspective of the field.
- **Comprehensive and up-to-date review.** Our survey presents an extensive and up-to-date review of 3D-GS, covering both classical and cutting-edge approaches. For each category, we provide fine-grained classification and concise summaries.
- **Insights into future directions in 3D-GS.** We highlight the technical limitations of current research and propose several promising avenues for future work, aiming to inspire further advancements in this rapidly evolving field. Special emphasis is given to exploring the potential roles of 3D-GS, offering insights into their future applications.

The structure of this survey is organized as follows: Section 2 provides an introduction to the background knowledge of 3D Gaussian Splatting. Section 3 presents a systematic review of the methods used to optimize 3D-GS, including considerations such as rendering efficiency, realism of the rendered images, costs, and the physics involved in 3D-GS. Additionally, Section 4 reviews recently proposed methods for reconstructing meshes, while Section 5 compares and summarizes the techniques employed for manipulating 3D-GS. Furthermore, Section 6 examines the methods for 3D generation from both object-level and scene-level perspectives. Moreover, Section 7 and Section 8 provide summaries of the applications of 3D-GS in perception and human body research, respectively. Finally, Section 9 identifies several promising future directions for 3D-GS.

2 Background

Gaussian Splatting Radiance Field. Gaussian Splatting Radiance Field [Kerbl et al., 2023] also referred to as 3D Gaussian Splatting(3DGS), is an explicit radiance field-based scene representation that represents a radiance field using a large number of 3D anisotropic balls, each modeled using a 3D Gaussian distribution (Eq. 1). More concretely, each anisotropic ball has mean $\mathcal{M} \in \mathbb{R}^3$, covariance Σ , opacity $\alpha \in \mathbb{R}$ and spherical harmonics parameters $\mathcal{C} \in \mathbb{R}^k$ (k is the degrees of freedom) for modeling view-dependent color. For regularizing optimization, the covariance matrix is further

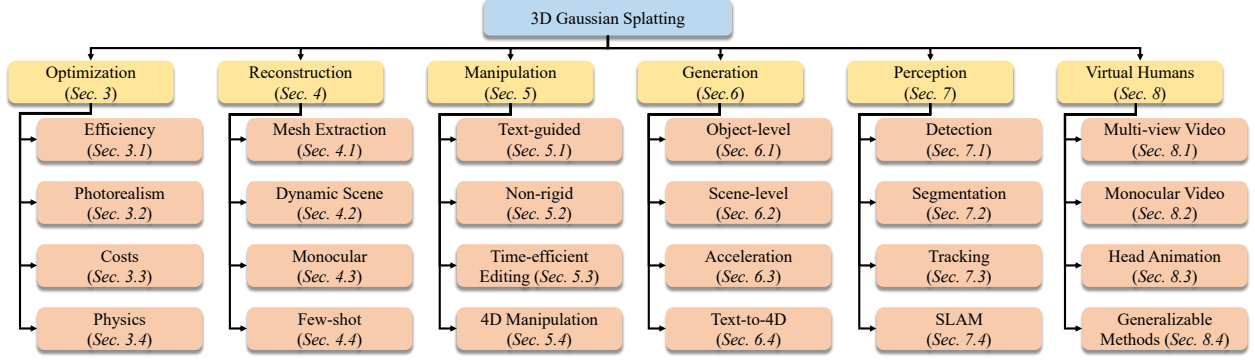


Figure 2: Taxonomy of existing 3D Gaussian Splatting derived methods.

decomposed into rotation matrix \mathbf{R} and scaling matrix \mathbf{S} by Eq 2. These matrices are further represented as quaternions $r \in \mathbb{R}^4$ and scaling factor $s \in \mathbb{R}^3$.

$$G(X) = e^{-\frac{1}{2}\mathcal{M}^T\Sigma^{-1}\mathcal{M}} \quad (1)$$

$$\Sigma = \mathbf{R}\mathbf{S}\mathbf{S}^T\mathbf{R}^T \quad (2)$$

For this scene representation, view rendering is performed via point splatting [Yifan et al., 2019]. Specifically, all Gaussian balls in the scene are first projected onto the 2D image plane, and their color is computed from spherical harmonic parameters. Then, for every 16×16 pixel patch of the final image, the projected Gaussians that intersect with the patch are sorted by depth. For every pixel in the patch, its color is computed by alpha compositing the opacity and color of all the Gaussians covering this pixel by depth order, as in Eq. 3.

$$C = \sum_{i \in N_{\text{cov}}} c_i \alpha_i \prod_{j=1}^{i-1} (1 - \alpha_j) \quad (3)$$

where, N_{cov} represents the splats that cover this pixel, α_i represents the opacity of this Gaussian splat multiplied by the density of the projected 2D Gaussian distribution at the location of the pixel, and c_i represents the computed color.

Datasets. Various publicly available datasets are utilized to evaluate the performance of 3D-GS on various tasks. Table 1 provides an overview of some of these datasets for 3D-GS in optimization, reconstruction, manipulation, generation, perception, and the human body.

Table 1: List of commonly used datasets for 3D Gaussians.

Dataset	Year	Samples	Camera Views	Type	Description	Task
Mip-NeRF 360 [Barron et al., 2022]	CVPR'22	9	360 viewpoint	Videos	Outdoor and indoor scene containing a complex central object or area with a detailed background	Optimization & Reconstruction
Tanks and Temples [Knapitsch et al., 2017]	ToG'17	14	263-1107	Videos	Ground-truth captured by high quality industrial laser scanner	Optimization & Reconstruction
DeepBlending [Hedman et al., 2018]	TOG'18	19	12-418	Images	Images with sufficient variety of scene content	Optimization & Reconstruction
Plenoptic Video [Li et al., 2022]	CVPR'22	6	21	Videos	Captured daily events with challenging scene motions	Optimization & Reconstruction
D-NeRF [Pumarola et al., 2021]	CVPR'21	8	360 viewpoint	Synthetic videos	Animated objects with complex geometries and non-Lambertian materials	Optimization & Manipulation
DyNeRF	CVPR'22	6	20	Videos	Time-synchronized and calibrated multi-view videos that covers challenging 4D scenes	Optimization
NeRF-LLFF [Mildenhall et al., 2019]	SIGGRAPH'19	8	forward-facing views	images	A subset of Real Iconic	Optimization
RealEstate10k [Zhou et al., 2018]	ToG'18	about 80k	-	Videos	Video clips on YouTube shot from a moving camera	Reconstruction
ACID [Liu et al., 2021]	ICCV'21	765	-	Videos	A dataset of aerial landscape videos	Reconstruction
ShapeNet [Chang et al., 2015]	2015	about 60k	50	Synthetic images	A richly-annotated, large-scale dataset of 3D shapes	Reconstruction
Tensor4D [Shao et al., 2023a]	CVPR'23	4	1, 4, 12	Videos	Dynamic half-body human videos by four sparsely positioned, fixed RGB cameras	Manipulation
Nerf-DS [Pumarola et al., 2021]	CVPR'23	7	2 forward-facing views	Videos	Dynamic specular dataset	Manipulation
CoNeRF [Kania et al., 2022]	CVPR'22	7	-	Videos	Real face scenes	Manipulation
InterHand2.6M [Moon et al., 2020]	ECCV'20	36	80-140	Videos	2.6M labeled single and interacting hand frames	Manipulation
NVOS [Ren et al., 2022]	ICCV'22	7	20-62	Images	Real-world front-facing scenes with annotated object masks based on LLLFF	Perception
SPIn-NeRF [Mirzaei et al., 2023]	CVPR'23	10	100	Images	Real-world front-facing scenes with human annotated object masks	Perception
LERF [Ker et al., 2023]	ICCV'23	13	-	Videos	A mixture of in-the-wild and posed long-tail scenes	Perception
Replica [Straub et al., 2019]	arXiv'19	18	-	Videos	Highly photo-realistic 3D indoor scene dataset at room and building scale	Perception
KITTI [Geiger et al., 2012]	CVPR'12	22	-	Videos	A city-scale dataset created for autonomous driving research	Perception
Objaverse 1.0 [Deitke et al., 2023]	CVPR'23	818k	-	3D objects	A large dataset of over 800K 3D models with descriptive captions, tags, and animations.	Generation
OmniObject3D [Wu et al., 2023b]	CVPR'23	6k	-	3D objects	Real-scanned 3D object captured with both 2D and 3D sensors, providing textured meshes, point clouds, multi-view rendered images, and multiple real-captured videos.	Generation & Perception & Reconstruction
People-Snapshot [Alldieck et al., 2018]	CVPR'18	24	1	Videos	Containing subjects captured with varying sets of garments and with three different background scenes	Virtual Humans
DynaCap [Habermann et al., 2021]	ToG'21	5	50-101	Videos	Recording 5 subjects wearing different types of apparel and performing a wide range of motions like "dancing"	Virtual Humans
ZJU-Mocap [Peng et al., 2021]	CVPR'21	9	21	Videos	9 dynamic human videos with 60 to 300 frames	Virtual Humans
THuman4 [Zheng et al., 2022]	CVPR'22	3	24	Videos	multi-view human videos ranging from 2500 to 5000 frames	Virtual Humans
NeuMan [Jiang et al., 2022]	ECCV'22	6	1	Videos	Monocular videos featuring a single individual	Virtual Humans
ActorsHQ [Isik et al., 2023]	arXiv'23	16	160	Videos	captured using a mobile phone	Virtual Humans
					Containing 8 actors with casual clothing such as skirts or shorts	Virtual Humans

3 Optimization of Gaussian Intrinsic Properties

Despite the already showcased capability and efficiency of 3D Gaussian Splatting, there is still room for further refinement in the following promising directions (as depicted in Fig 3): (a) Making 3D-GS more memory efficient is critical for real-time rendering; (b) The quality of rendered image could be further enhanced; (c) Reducing the costs of images for synthesizing novel views; (d) Enabling 3D Gaussians to represent dynamic scenes with faithful dynamics.

3.1 Efficiency

The parameters within millions of Gaussians that represent the scene require an enormous memory space for storage, hence the reduction of memory usage while maintaining quality is critical and beneficial for real-time rendering.

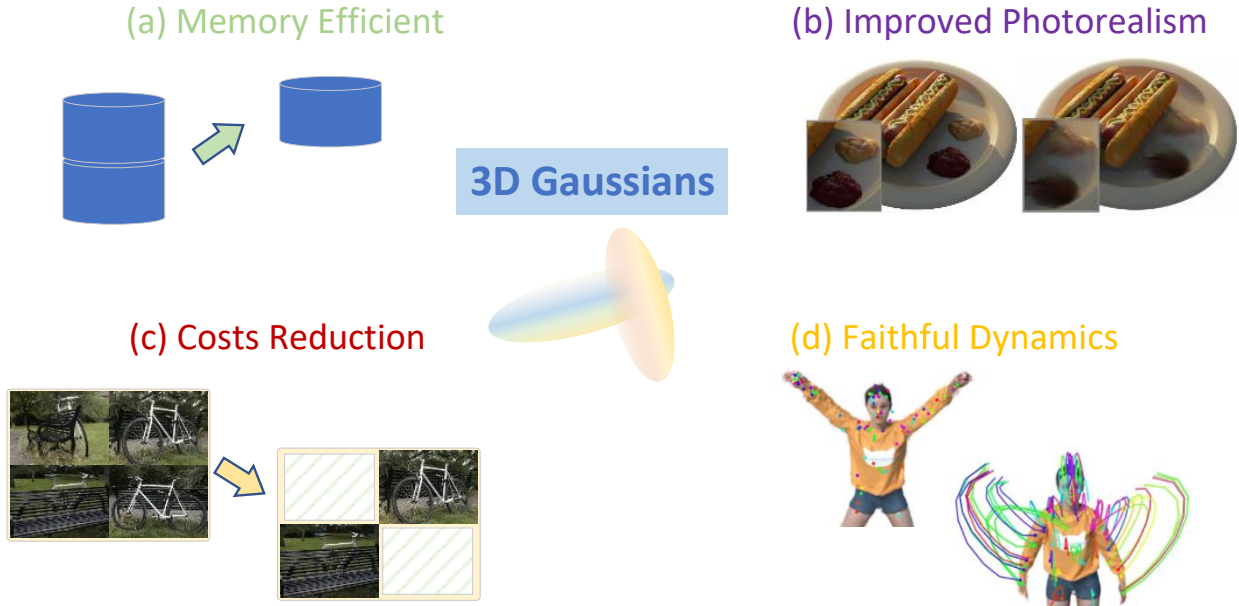


Figure 3: An illustration of optimizing 3DGS: (a) efficiency, (b) photorealism, (c) costs, and (d) physics. Images courtesy of [Jiang et al., 2023a, Kratimenos et al., 2023, Zhu et al., 2023].

Encouraged by the grid-guided NeRF, Lu et al. [Lu et al., 2023] proposed Scaffold-GS that is memory efficient while maintaining comparable rendering quality and speed. Scaffold-GS exploits underlying scene structure to help prune excessively expanded Gaussian balls. It utilizes initialized points from Structure-from-motion [Schonberger and Frahm, 2016] to construct a sparse grid of anchor points, to each of which a set of learnable Gaussians is attached. Attributes of these Gaussians are predicted on-the-fly according to specific anchor features. Furthermore, a policy guided by the aggregated gradients of the neural Gaussians is adopted to grow anchor points wherever significant and trivial anchors are eliminated by a pruning operation. An additional volume regularization loss term [Lombardi et al., 2021] is added in order to encourage the Gaussians to be small with minimal overlapping.

Vector quantization (VQ) technique [Equitz, 1989] is a method utilized for data compression and encoding. It involves categorizing data into clusters of similar vectors and then representing them using a codebook that describes these vectors. This approach facilitates efficient storage and transmission of data. Therefore, Navaneet et al. [Navaneet et al., 2023] proposed CompGS to drastically reduce the memory required for 3D-GS. CompGS adopts vector quantization to compress the parameters of 3D Gaussians. Specifically, K-means is performed on the color, spherical harmonics, scale, and rotation vectors separately to obtain relative clusters for efficient quantization. The opacity and position parameters are left untouched since the former is a plain scalar and the quantization of the latter will cause overlapping of Gaussians. Furthermore, the indices of codebooks are represented in fewer bits, and the Gaussians are sorted based on their color so that only one index is stored for the first Gaussian of one color and the rest with identical color simply subsequently adds 1. Meanwhile, Girish et al. [Girish et al., 2023] introduced EAGLES to improve memory usage efficiency for 3D-GS. EAGLES utilizes a set of quantized representations for the attribute vectors of Gaussians. Specifically, except for the coefficient of base band color spherical harmonics and scaling, and position vectors, all other attributes are quantized and encoded. The continuous approximations are maintained for the back-propagation of gradients. Attributes are then retrieved from the latent quantized vectors via an MLP decoder. Furthermore, EAGLES

utilizes a coarse-to-fine training strategy that gradually increases the rendering size. This leads to reduced training times and improved final quality.

On the other hand, the lossless octree-based algorithm is also utilized. For instance, Fan et al. [Fan et al., 2023] proposed LightGaussian to compress Gaussians for memory efficiency. It first evaluates the global significance of each Gaussian according to its contribution to each pixel from all training views. The calculated scores are then utilized to prune insignificant Gaussians. The degree of coefficients of spherical harmonics are reduced via data distillation and coefficients of trivial Gaussians are quantized to save storage space. Pseudo-views are randomly sampled to facilitate the knowledge transfer. Furthermore, the position parameter is compressed via a lossless octree-based algorithm and the remaining attributes are saved in half-precision format for further memory saving.

Moreover, Katsumata et al. [Katsumata et al., 2023] proposed to relieve the memory required for 3D Gaussian dynamic scene representation. It divides the parameters of Gaussians into time-invariant and time-varying ones. The former contains the position and rotation which are estimated via Fourier and linear approximation respectively. This approach effectively reduces memory consumption when compared to storing each of those parameters in every time step. Furthermore, the flow information is employed via a loss term to overcome the ambiguity between consecutive frames across different time steps.

Challenges: Representing scenes with intricate details requires an enormous amount of 3D Gaussians. The tremendous storage space needed for Gaussians not only impedes its application on edge devices but also restrains the rendering speed.

Opportunities: Existing vector quantization and pruning of insignificant Gaussian methods have demonstrated their effectiveness in compressing 3D Gaussians for static scenes. However, extending them to dynamic scenes and improving the compactness of dynamic representation are still underexplored.

3.2 Photorealism

The aliasing issue and artifacts emerge during the splatting process and resolving them is clearly favorable for the quality and realness of rendered image. Besides, the realness of reflections within the scene could be further improved.

Yan et al. [Yan et al., 2023a] introduced a multi-scale approach for mitigating aliasing effect in 3DGS. They postulate that such an issue is primarily caused by the splatting of large amounts of Gaussians filled in regions with intricate 3D details. Hence, they propose to represent the scene at different levels of detail. For each level, small and fine-grained Gaussians below a certain size threshold in each voxel are aggregated into larger Gaussians and then inserted into subsequent coarser levels. These multi-scale Gaussians effectively encode both high- and low-frequency signals and are trained with original images and their downsampled counterparts. During the rendering process, Gaussians with appropriate scale are selected accordingly which results in an improvement of quality and increasing in rendering speed.

Mip-Nerf [Barron et al., 2022] is proven as an efficient and robust method in the field of Nerf. Encouraged by Mip-Nerf, Yu et al. [Yu et al., 2023a] introduced 3D smoothing and 2D Mip filters to resolve ambiguities within the optimization process of 3D Gaussians. Derived from the Nyquist-Shannon Sampling Theorem [Nyquist, 1928, Shannon, 1949], the 3D filter performs as a Gaussian low-pass filter that restrains the frequency of 3D representation within half of the maximal sampling rate, which derived from multi-view images, to remove high-frequency artifacts. On the other hand, 2D filter aims to mitigate the aliasing issue when rendering reconstructed scenes at a lower sampling rate. It replaces the screen space dilation filter of 3D-GS and replicates the behavior of a box filter from the physical imaging process [Mildenhall et al., 2022, Szeliski, 2022]. This principled approach achieves better generalization to out-of-distribution scenarios with unseen camera poses and zoom factors.

Except for the improvement of rendering details, lightness decomposition is also an urgent challenge to be solved since the original 3D-GS works not very well on specific materials. Gao et al. [Gao et al., 2023] introduced a framework for photo-realistic rendering. It utilizes a set of relightable 3D Gaussian points to represent the scene. The surface normal is regularized by the consistency between the rendered normal and the pseudo normal which is computed from the rendered depth map. Geometry clues are introduced via the integration of Multi-View Stereo cues [Yao et al., 2018]. This approach adopts a simplified Disney BRDF model [Yao et al., 2022] and assigns extra properties to each Gaussian for rendering. The incident light is divided into local and global components that are represented by spherical harmonics of each Gaussian and shared global spherical harmonics multiplied by a visibility term respectively. In order to improve the rendering efficiency and quality, the physical-based rendering color is computed at Gaussian level and additional regularization terms are attached to the optimization process. Moreover, inspired by [Karras, 2012], a novel ray tracing technique based on the Bounding Volume Hierarchy is introduced to further enhance the realness of rendering. Jiang et al. [Jiang et al., 2023a] proposed GaussianShader to further enhance the realism of scenes with specular features and reflective surfaces. GaussianShader explicitly considers the light-surface interaction and incorporates a simplified

approximation of the rendering equation [Kajiya, 1986] for high-quality rendering with considerably lower time cost. In order to accurately predict normals on discrete 3D Gaussians, the shortest axis is selected as the approximated normal and two additional trainable normal residuals are introduced for regularization, one for outward and the other for inward axis scenarios. Furthermore, consistency of normal-geometry is enforced by minimizing the difference between the grad normals derived from rendered depth maps and rendered normals maps using previously predicted normals. Liang et al. [Liang et al., 2023a] presented GS-IR that introduces 3D-GS to inverse rendering. GS-IR first generates depth and improves it by considering the depth as a linear interpolation of the distances from 3D Gaussians to the image plane. Then the pseudo normals are derived by leveraging the calculated depth and are tied to the depth gradient normal via L_1 regularization. The indirect illumination is modeled by a spherical harmonics-based architecture and the occlusion information is pre-computed and cached. Finally, GS-IR adopts differentiable splatting along with a physic-based rendering pipeline, and split-sum approximation [Karis and Games, 2013] is utilized to mitigate the intractable integrals. Li et al. [Ma et al., 2023] proposed SpecNeRF that improves the modeling of specular reflections especially for near-field lighting conditions. Different from aforementioned methods that ameliorate reflection based on 3D-GS, SpecNeRF aims to enhance the ability of NeRF by incorporating 3D Gaussians as a novel directional encoding. It utilizes a set of learnable Gaussians as the basis to embed a 5D ray space that includes the ray origin and ray direction. Therefore, the encoding function could vary spatially and the change of spatial features aligns with the behavior of specular components. This results in a better modeling of reflections and improves the realness. SpecNeRF also introduced an initialization stage which involves refinement of Gaussian Parameters to facilitate the joint optimization of the Gaussians and NeRF. Additionally, the monocular normals estimated via a prior model [Eftekhari et al., 2021] are utilized in the early training stage to provide a supervised signal for the predicted normals and mitigate the shape-radiance ambiguity.

Challenges: Although the projection of 3D Gaussians onto 2D image drastically accelerates the rendering process, it complicates the calculation of occlusion which leads to poor estimation of illumination. In the meantime, the under-regularized 3D-GS fails to capture precise geometry and cannot natively generate accurate normals. Furthermore, the aliasing issue and artifacts deteriorate the quality of rendered images especially when synthesizing for unseen camera views.

Opportunities: View-dependent variations are critical for scenes featuring specular objects and complex reflections. Hence, empowering 3D-GS to capture significant appearance properties is beneficial for enhancing the realness of rendering. To better reduce the aliasing effects, it is worth investigating methods for more effective elimination of redundant Gaussians without compromising its expressive capability. Besides, the lack of rigorous normal estimation and geometry regularization which impedes the amelioration of image quality could be further compensated.

3.3 Costs

To synthesize novel views with high quality, the amount of required images is tremendous. Loosening this limitation is desirable for further exploring the potential of 3D-GS.

Several works have been proposed to solve the few-shot problem in 3D-GS. Chung et al. [Chung et al., 2023a] introduced a depth-regularized approach to avoid overfitting in few-shot image synthesis. Geometry constraints are introduced by exploiting both sparse and dense depth maps obtained from COLMAP [Schonberger and Frahm, 2016] and a monocular depth estimation model respectively. To prevent overfitting, this approach adopts unsupervised constraint for geometry smoothness [Godard et al., 2017] and utilizes Canny edge detector [Canny, 1986] to avoid regularization in edge areas where depth varies significantly. Furthermore, the maximum degree of spherical harmonics is restricted to 1 and an early stop optimization strategy is used to further reduce the overfitting. Zhu et al. [Zhu et al., 2023] proposed FSGS for novel view synthesis under limited observations. FSGS adopts a similar idea from vertex-adding strategy [Zorin et al., 1996] and gradually grows the initialized 3D Gaussians that are derived from Structure-from-Motion [Schonberger and Frahm, 2016] to fill the scene. The sparse Gaussians are utilized to construct a directed proximity graph that connects the nearest K neighbors and the proximity score of each Gaussian is subsequently calculated from the average distance to its neighbors. FSGS then proposes proximity-guided Gaussian unpooling to densify Gaussians and exploit Pearson correlation loss to provide a soft constraint between the rendered depth map and the depth map estimated via a well-trained monocular depth estimator. Additionally, FSGS employs pseudo-view augmentation through a 2D prior model to mitigate the issue of overfitting to sparse training views. Xiong et al. [Xiong et al., 2023] introduced SparseGS which boosts the performance of 3D-GS for few-shot view synthesis. Similar to prior works [Long et al., 2022], SparseGS adopts a depth map for regularization and proposes to apply an additional pre-trained depth estimation model [Lasinger et al., 2019, Miangoleh et al., 2021] for computing a patch-based Pearson correlation between the two depth loss terms. The absence of images for uncovered regions is compensated by utilizing a generative diffusion model and 3D-GS is guided via Score Distillation Sampling [Poole et al., 2022]. Furthermore, SparseGS devises a

pruning strategy that identifies the parts of a rendered image that suffer from floating artifacts or background collapse and removes them to improve the quality of the synthesized image.

Challenges: The performance of 3D-GS heavily relies on the quantity and accuracy of initialized sparse points. This default initialization method naturally contradicts the aim of image cost reduction and makes it grueling to achieve. Besides, inadequate initialization could cause overfitting and yield over-smoothed results.

Opportunities: Employing an additional monocular depth estimation model could provide useful geometry priors to adjust 3D Gaussians for effective coverage of the scene. However, this strong dependency on the estimation accuracy could lead to poor reconstruction of scenes with complex surfaces where the model fails to output accurate prediction. It is promising to further explore methods for effective densification and adjustment of 3D Gaussians and sufficient utilization of geometry information to improve the rendering quality.

3.4 Physics

It is beneficial to enhance the ability of 3D Gaussians by extending them from representing static scenes to 4D scenarios that could incorporate faithful dynamics that align with real-world physics.

In dynamic scenes, learning deformation is more convenient than modeling scenes at every time step. Wu et al. [Wu et al., 2023a] proposed a novel framework for real-time 3D dynamic scene rendering. Instead of directly constructing 3D Gaussians for each time-stamp with excessive memory costs, their framework first employs a spatial-temporal encoder that utilizes multi-resolution K-Planes [Fridovich-Keil et al., 2023] and MLP for effective feature extraction. The compact multi-head MLPs then perform as the decoder and separately predict the deformation of the position, rotation, and scaling of 3D Gaussians based on the input feature. This approach learns the Gaussian deformation field that leads to efficient memory usage and fast convergence. Meanwhile, Duisterhof et al. [Duisterhof et al., 2023] introduced MD-Splatting to perform 3D point tracking while synthesizing dynamic novel views. MD-Splatting adopts a feature encoding technique [Wu et al., 2023a, Cao and Johnson, 2023] and learns the Gaussian deformation in a metric space rather than a non-metric canonical one. The opacity and scale parameters are not inferred since learning them over time would allow Gaussians to disobey the accurate motion of points. Furthermore, the rigidity and isometry losses from [Luiten et al., 2023] along with a conservation of momentum loss are incorporated to regularize the trajectory.

Kratimenos et al. [Kratimenos et al., 2023] presented DynMF to synthesize dynamic views in a real-time fashion. DynMF decomposes complex motions within a given scene into a few basis trajectories from which each point or motion can be adequately derived. The trajectories are then predicted through an MLP which inherently forms a motion neural field. The sharing of neural basis across all points yields physically plausible and frame-consistent sequences. To prevent the selection of unnecessary basis and enforce strict sparsity, DynMF adopts a stronger loss term that forces each Gaussian to choose only a few trajectories.

Yang et al. [Yang et al., 2023a] proposed 4DGS to model space and time as an entirety to address general dynamic scene representation and rendering. 4DGS extends the scaling and rotation matrix that is decomposed from the original covariance matrix [Kerbl et al., 2023] to 4D Euclidean space. The derived general 4D Gaussian representation achieves reasonable fitting to 4D manifold while capturing the underlying dynamics of the scene. Additionally, 4DGS allows the appearance to vary with viewpoint and colors to evolve through time by exploiting the spherindrical harmonics, realizing a more faithful rendering of the dynamic scenes from the real world.

Xie et al. [Xie et al., 2023] introduced PhysGaussian to seamlessly integrate physical simulation within 3D-GS for generating novel dynamics and views. PhysGaussian first reconstructs a static scene via 3D-GS and over-skinny Gaussians could be regularized via an optional anisotropic loss. The simulation of continuum mechanics is incorporated through a time-dependent continuous deformation map. Gaussian kernels are then treated as discrete particle clouds and simultaneously deform with the continuum. To enforce the deformed kernels under the deformation map to be a Gaussian, PhysGaussian utilizes the first-order approximation to characterize the particles undergoing local affine transformations. Additionally, the internal area of objects could be optionally filled via the 3D opacity field to assist in the rendering of exposed internal particles.

Challenges: The intrinsic sparsity of input point clouds poses an essential challenge for the reconstruction of scenes with faithful dynamics. It is even more challenging to capture physically plausible dynamics while maintaining the quality, for instance, rendering the change of shadows with high fidelity.

Opportunities: Objects with large motions could cause unnatural distortion among consecutive frames and incorporating neural networks with learned scene-specific dynamics could improve the fidelity of deformations. Current methods for reconstruction of dynamic scenes mainly focus on indoor object-level deformations and they still require images taken from multiple camera views along with the precise camera pose. Extending 3D-GS to larger dynamic scenes and relaxing such limitations are more than beneficial for real-world applications.

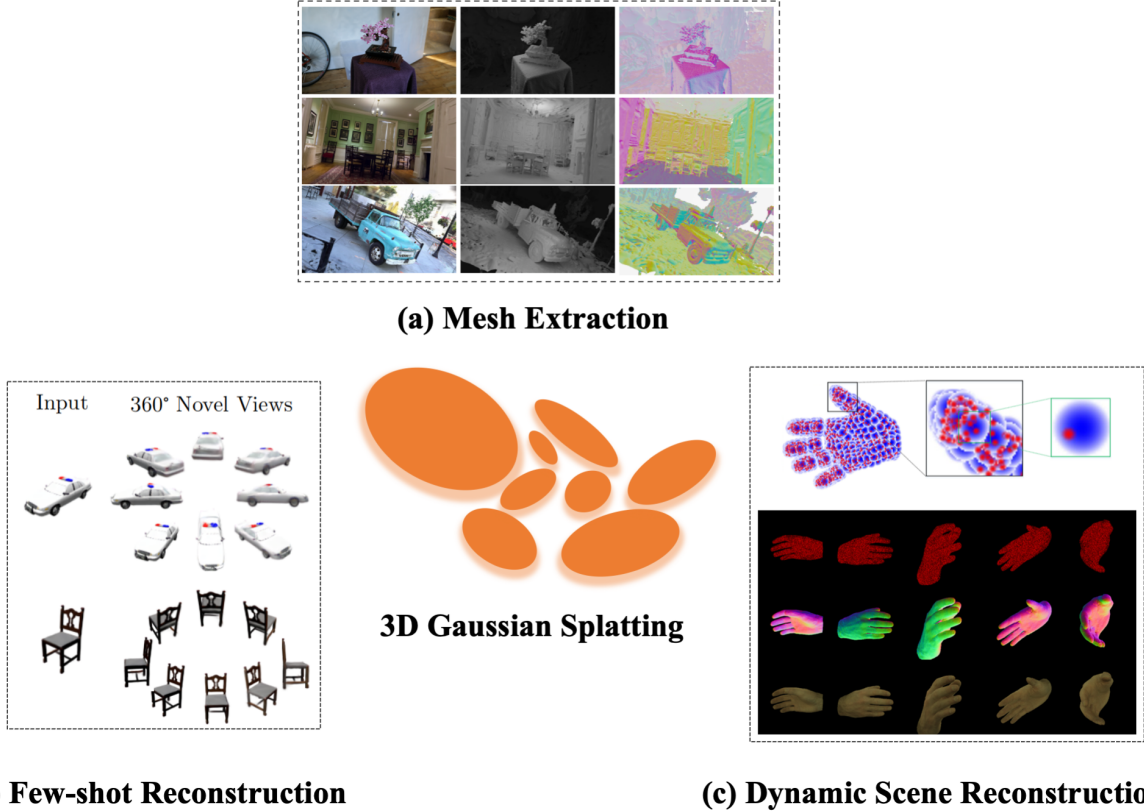


Figure 4: An illustration of 3D-GS on reconstruction: (a) Mesh extraction of 3D-GS, (b) few-shot reconstruction, and (c) dynamic scene reconstruction. Images courtesy of [Guédon and Lepetit, 2023, Szymanowicz et al., 2023, Jiang et al., 2023b].

4 Reconstruction

As previously mentioned, the widespread adoption of 3D-GS in the capture and rendering of 3D scenes from novel viewpoints can be attributed to its exceptional rendering speed and ability to produce realistic results. Similar to NeRFs, the extraction of surface meshes in 3D-GS (as shown in Fig.4a) is a fundamental yet essential aspect. Further investigation is necessary to tackle challenging scenarios, such as monocular or few-shot situations (as depicted in Fig.4b), which are commonly encountered in practical applications like autonomous driving. Additionally, the training times of 3D-GS are on the order of minutes, enabling real-time rendering and facilitating the reconstruction of dynamic scenes (as illustrated in Fig. 4c).

4.1 Surface Mesh Extraction

Surface mesh extraction poses a classic challenge in computer vision. However, the explicit representation of the scene through a 3D Gaussian distribution introduces a significant level of complexity to this task. Consequently, several novel methods have been proposed to effectively address this complexity and facilitate the extraction of surface meshes.

Guédon et al. [Guédon and Lepetit, 2023] introduced the SuGaR for 3D mesh reconstruction and high-quality mesh rendering. SuGaR incorporates a regularization term to promote alignment between the Gaussians and the scene’s surface. The Poisson reconstruction method is then used to leverage this alignment and derive a mesh from the Gaussians. To bind the Gaussians to the mesh surface, SuGaR presents an optional refinement strategy that optimizes both the Gaussians and the mesh using Gaussian splatting rendering. However, the mandatory restrictions on the Gaussians result in a decrease in rendering quality. Nevertheless, these restrictions lead to improved performance in mesh extraction. Meanwhile, Chen et al. [Chen et al., 2023a] introduced NeuSG that jointly optimizes NeuS [Wang et al., 2021] and 3D-GS to achieve highly detailed surface recovery. Similar to the regularization term in SuGaR [Guédon and Lepetit, 2023], NeuSG incorporates regularizers to ensure that point clouds generated from extremely thin 3D Gaussians closely

adhere to the underlying surfaces. This approach leverages the benefits of joint optimization, resulting in the generation of comprehensive surfaces with intricate details.

4.2 Monocular and Few-shot Reconstruction

The introduction of 3D-GS represents a promising advancement in monocular and few-shot reconstruction tasks. However, a significant challenge in these tasks is the absence of geometric information. Consequently, numerous studies have been devoted to addressing this challenge and proposing innovative methods to overcome the lack of geometric information in the perspective.

At first, the technique for few-shot 3D reconstruction allows for reconstructing 3D scenes with a limited amount of input data. Charatan et al. [Charatan et al., 2023] presented PixelSplat for 3D reconstruction from image pairs. The primary focus of PixelSplat is to address the challenge of scale factor inference by proposing a multi-view epipolar transformer. By utilizing scale-aware feature maps, PixelSplat presents a novel approach for predicting the parameters of a set of Gaussian primitives. The scene is parameterized through pixel-aligned Gaussians, enabling the implicit spawning or deletion of Gaussian primitives during training. This strategy helps avoid local minima while ensuring a smooth gradient flow. Notably, PixelSplat demonstrates exceptional performance in capturing intricate details and accurately inferring 3D structure, particularly in regions of the scene that are only observable from a single reference view. Zou et al. [Zou et al., 2023] utilized two transformer-based networks to perform single-view 3D object reconstruction using a hybrid representation named Triplane-Gaussian, which combines an explicit point cloud with an implicit triplane field. By incorporating local image features for projection-aware conditioning within the transformer networks, this method enhances consistency with the input observation. Triplane-Gaussian leverages both explicit and implicit representations, resulting in efficient and high-quality single-view reconstruction.

Monocular 3D reconstruction is capable of inferring the shape and structure of a 3D scene from 2D images using a single camera. The key to monocular 3D reconstruction involves the meticulous analysis of perspective relationships, textures, and motion patterns within the images. By employing monocular techniques, it becomes possible to accurately estimate the distances between objects and discern the overall shape of the scene. Szymanowicz et al. [Szymanowicz et al., 2023] introduced Splatter Image, an ultra-fast approach for monocular 3D object reconstruction. This approach utilizes a 2D CNN architecture to efficiently process images, predicting a pseudo-image where each pixel is represented by a colored 3D Gaussian. Splatter Image demonstrates rapid training and evaluation on both synthetic and real benchmarks without the need for canonical camera poses. Furthermore, it is also capable of few-shot 3D reconstruction by incorporating cross-view attention. Das et al. [Das et al., 2023] introduced Neural Parametric Gaussians (NPGs) for reconstructing dynamic objects from monocular videos. This method employs a two-stage reconstruction approach: first, learning coarse deformation and using it as a constraint for the reconstruction in the second stage. In the initial stage, a coarse parametric point model is implemented based on a low-rank deformation, providing regularization and temporal correspondences for object reconstruction. The second stage involves optimizing 3D Gaussians, anchored in and deformed by locally oriented volumes. NPGs significantly improve non-rigid novel view synthesis from a monocular camera, particularly in challenging scenarios with limited multi-view cues.

4.3 Dynamic Scene Reconstruction

The high rendering speed and resolution of 3D-GS support dynamic scene reconstruction, including human body tracking and large urban scene reconstruction.

Lin et al. [Lin et al., 2023] introduced Gaussian-Flow based on 3D-GS for swift dynamic 3D scene reconstruction and real-time rendering, which facilitates the segmentation, editing, and composition of both static and dynamic 3D scenes. This approach introduces the Dual-Domain Deformation Model (DDDM) to capture the time-dependent residual of each attribute through polynomial fitting in the time domain and Fourier series fitting in the frequency domain. Gaussian-Flow is able to eliminate the need for training separate Gaussians for each frame or introducing an additional implicit neural field to model 3D dynamics.

Yang et al. [Yang et al., 2023b] proposed a deformable 3D-GS method for reconstructing scenes by utilizing 3D Gaussians learned in canonical space with a deformation field to model monocular dynamic scenes. This method incorporates an annealing smoothing training mechanism to mitigate the influence of inaccurate poses on the smoothness of time interpolation tasks in real-world datasets. This approach attains real-time rendering and high-fidelity scene reconstruction in dynamic scenes.

Jiang et al. [Jiang et al., 2023b] introduced 3D-PSHR for real-time dynamic hand reconstruction. 3D-PSHR incorporates a self-adaptive canonical points upsampling strategy and self-adaptive deformation, enabling pose-free hand

reconstruction. Furthermore, for texture modeling, 3D-PSHR separates the appearance color into intrinsic albedo and pose-aware shading based on normal deformation, both of which are acquired through a Context-Attention module.

Chen et al. [Chen et al., 2023b] employed the 3D-GS and introduced a unified representation model named Periodic Vibration Gaussian (PVG) to address the challenge of modeling large-scale scenes with intricate geometric structures and unconstrained dynamics. PVG extends the 3D Gaussian Splatting paradigm to seamlessly integrate periodic vibration-based temporal dynamics and devises innovative mechanisms for improved temporal continuity and adaptive control. PVG demonstrates superior performance in both the reconstruction and novel view synthesis of dynamic and static scenes, all without relying on manually labeled object bounding boxes or expensive optical flow estimation.

Challenges: As 3D-GS is an explicit representation model for reconstruction, each Gaussian kernel may not necessarily lie on the surface of a certain object, raising a challenge for surface mesh extraction. There is a need to constrain the Gaussian kernel to adhere to the object’s surface, but this might lead to a reduction in rendering accuracy.

Opportunities: (i) For few-shot reconstruction, integrating with a diffusion model or eliminating the requirement for camera poses could facilitate large-scale training. (ii) Additionally, for surface mesh extraction, introducing the method of lighting decomposition may extract more realistic surface textures. (iii) In dynamic scene reconstruction, prioritizing the optimization of the balance between speed and the preservation of image details may prove to be considerable.

5 Manipulation

Due to the explicit property of 3D-GS, it has a great advantage for editing tasks as each 3D Gaussian exists individually (Fig. 5). It is easy to edit 3D scenes by directly manipulating 3D Gaussians with desired constraints applied.

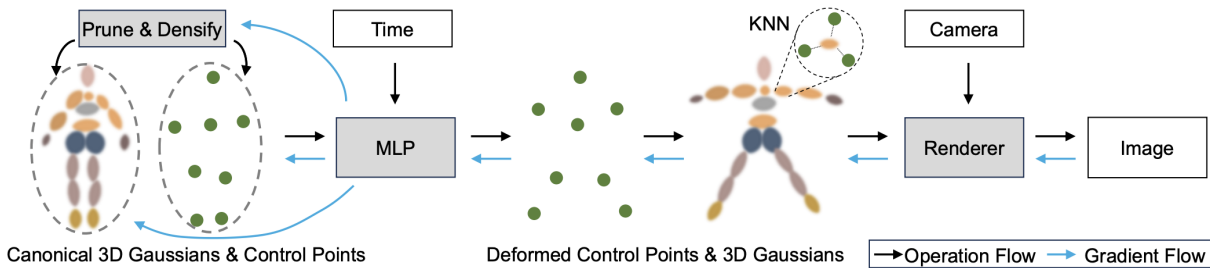


Figure 5: An illustration of employing sparse control points and a deformation MLP to direct 3D Gaussian dynamics. Images courtesy of [Huang et al., 2023a].

5.1 Text-guided Manipulation

In recent years, there has been a surge in the number of text-guided manipulation [Canfes et al., 2023, Yu et al., 2023b, Hwang et al., 2023]. Consequently, text-guided manipulation has garnered increased attention due to its proximity to human speech. Furthermore, as access to large language models becomes more widespread, the utilization of LLM-guided manipulation holds great promise as a future direction. Fang et al. [Fang et al., 2023] presented GaussianEditor for precise editing of 3D scenes using 3D Gaussians and text instructions. The first step involves extracting the region of interest (RoI) that corresponds to the provided text instruction and aligning it with the 3D Gaussians. This Gaussian RoI is then utilized to control the editing process, enabling fine-grained adjustments.

5.2 Non-rigid Manipulation

Non-rigid objects can change and deform in shape, enabling more realistic simulations of soft objects, biological tissues, and fluids. These objects offer several advantages, including increased authenticity and improved depiction of object deformation and behavior [Tretschk et al., 2021]. Moreover, these models allow for diverse effects as they can respond to external forces and constraints by deforming [Lazova et al., 2023]. However, non-rigid objects also present certain challenges. They are characterized by their complexity, necessitating careful consideration of factors such as object deformation, continuity, and collision during both editing and simulation. Additionally, the real-time interaction performance of non-rigid objects may be limited in applications, particularly when dealing with large-scale and complex non-rigid objects [Xu and Harada, 2022].

Pokhariya et al. [Pokhariya et al., 2023] introduced an articulated 3D Gaussian representation. Specifically, they proposed the development of MANUS-Hand for articulated hands, which leverages 3D Gaussian splatting to achieve

precise shape and appearance representation. In addition, they introduced MANUS to combine MANUS-Hand with a 3D Gaussian representation of the object to model contacts accurately. They also introduced MANUS-Grasps, an extensive real-world multi-view RGB grasp dataset. This dataset comprises over 7 million frames captured by 53 cameras, providing comprehensive 360-degree coverage of more than 400 grasps across various everyday life scenarios. The accuracy of contacts is validated by utilizing paint transfer between the object and the hand. Lei et al. [Lei et al., 2023] introduced GART for non-rigid articulated subjects. GART approximates the radiance field of the canonical shape and appearance using a Gaussian Mixture Model. Additionally, GART can be effectively animated through a learnable forward skinning technique. This representation is capable of capturing complex deformations, including loose clothing on human subjects.

Gao et al. [Gao et al., 2024] introduced a novel approach called mesh-based Gaussian Splatting for representing 3D Gaussians. This technique effectively combines the mesh representation with 3D Gaussians, leveraging the mesh to guide the splitting process and enhancing the overall quality of the learned GS. By employing Gaussian representation, they propose a Gaussian deformation method on a large scale. This method not only utilizes vertex positions but also incorporates deformation gradients to guide the GS. By taking advantage of mesh deformation methods, this approach ensures real-time rendering and robustly maintains a high-quality appearance even under substantial deformations.

5.3 Time-efficient Editing

While 3DGS is indeed a rapid rendering technique, it is crucial for it to operate in real-time during the editing of 3D Gaussians. Consequently, there is an urgent need to develop editing methods for 3DGS that are time-efficient.

Huang et al. [Huang and Yu, 2023] proposed Point’n Move, which enables interactive manipulation of scene objects through exposed region inpainting. The interactivity is enhanced by intuitive object selection and real-time editing. To achieve this, they took advantage of the explicit nature and speed of the Gaussian Splatting Radiance Field. The explicit representation formulation allows for the development of a dual-stage self-prompting segmentation algorithm, where 2D prompt points are used to create 3D masks. This algorithm facilitates mask refinement and merging, minimizes changes, provides a good initialization for scene inpainting, and enables real-time editing without the need for per-editing training. At the same time, Chen et al. [Chen et al., 2023c] introduced GaussianEditor for 3D editing that employs Gaussian Splatting to augment control and efficiency throughout the editing procedure. GaussianEditor employs Gaussian semantic tracing to accurately identify and target specific areas for editing. It then utilizes Hierarchical Gaussian Splatting (HGS) to strike a balance between fluidity and stability, resulting in detailed outcomes guided by stochastic principles. Moreover, GaussianEditor includes a specialized 3D inpainting algorithm for Gaussian Splatting, which streamlines the removal and integration of objects and significantly reduces editing time.

5.4 4D Manipulation

The field of 4D scene reconstruction has experienced notable progress with the introduction of dynamic neural 3D representation. These advancements have greatly improved the capacity to capture and depict dynamic scenes. However, despite these breakthroughs, the interactive editing of these 4D scenes continues to present significant obstacles. The main challenge lies in guaranteeing spatial-temporal consistency and maintaining high quality during 4D editing, while also providing interactive and advanced editing capabilities.

Shao et al. [Shao et al., 2023b] introduce Control4D for editing dynamic 4D portraits using text instructions. Control4D aims to overcome the challenges commonly encountered in 4D editing, particularly the limitations of existing 4D representations and the inconsistent editing outcomes resulting from diffusion-based editors. GaussianPlanes was first proposed as a novel 4D representation, which enhances the structure of Gaussian Splatting through plane-based decomposition in both 3D space and time. This approach improves the efficiency and robustness of 4D editing. Additionally, a 4D generator is leveraged to learn a more continuous generation space from the edited images produced by the diffusion-based editor, effectively enhancing the consistency and quality of 4D editing. Huang et al. [Huang et al., 2023a] proposed to model scene motion using sparse control points in conjunction with an MLP. They leverage the understanding that motions within a scene can be effectively represented by a compact subspace comprising a sparse set of bases. To facilitate the accurate learning of appearances, geometry, and motion from monocular videos, adaptive learning strategies are employed, along with the incorporation of a regularization loss that enforces rigid constraints. By adopting this sparse motion representation, this method enables motion editing by manipulating the learned control points while preserving high-fidelity appearances. Yu et al. [Yu et al., 2023c] introduced Controllable Gaussian Splatting (CoGS) for dynamic scene manipulation. Unlike NeRFs and other neural methods, CoGS utilizes an explicit representation, allowing for real-time and controllable manipulation of dynamic scenes. The explicit nature of CoGS not only enhances rendering efficiency but also simplifies the manipulation of scene elements.

Challenges: Firstly, in text-guided manipulation, the selection of Regions of Interest (RoIs) relies on the performance of segmentation models, which are influenced by noises. Secondly, when editing 3D Gaussians, several important physical aspects are often overlooked. Lastly, there is still room for improvement in achieving frame consistency in 4D editing.

Opportunities: i) In the manipulation of 3D-GS, existing 2D diffusion models encounter difficulties in providing adequate guidance for intricate prompts, resulting in constraints when it comes to 3D editing. Therefore, efficient and accurate 2D diffusion models can be utilized as better guidance for editing 3D Gaussians. ii) Existing methods have primarily been tested with minimal motion changes and accurate camera poses. Expanding their applicability to scenarios involving intense movements remains an area of investigation.

6 Generation

Thanks to the significant progress made in diffusion models and 3D representations, generating 3D assets from text/image prompts is now a promising task in AIGC domain. Furthermore, resorting to 3D-GS as the explicit representation of the object (Fig. 6a) and the scene (Fig. 6b) makes fast or even real-time rendering possible. Besides, some works focus on improving the time-consuming optimization process inherent in the Score Distillation Sampling (SDS) pipeline (Fig. 6c). While 3D generation has shown some impressive results, 4D generation (Fig. 6d) remains a challenging and underexplored topic.

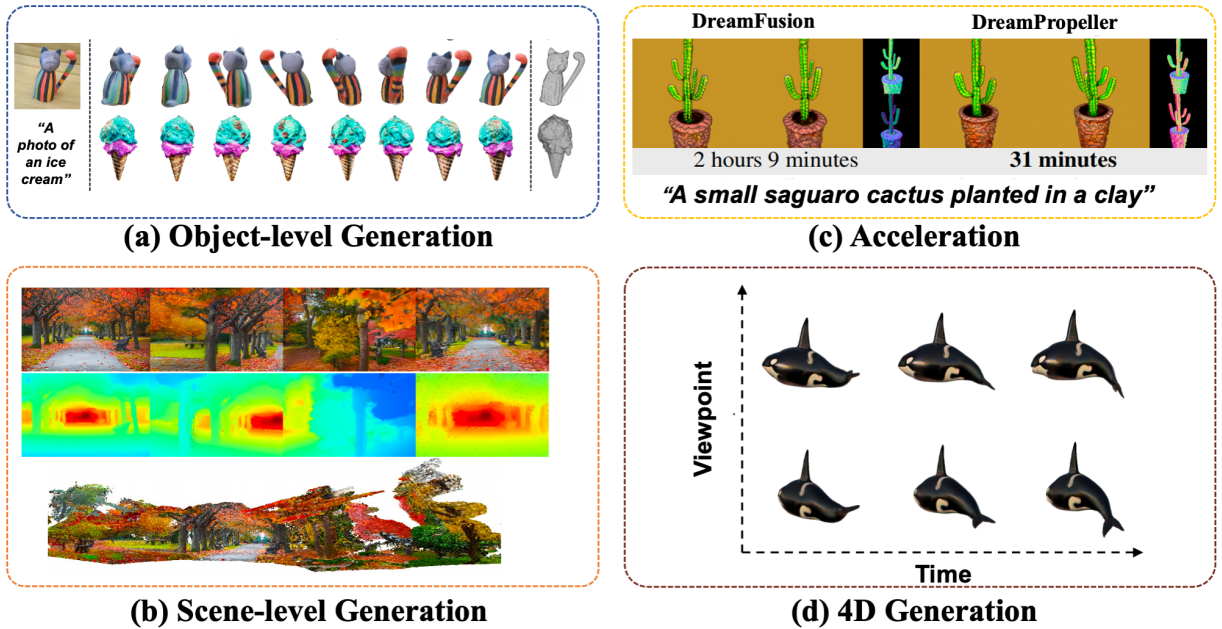


Figure 6: An illustration of 3D-GS on generation tasks: (a) object-level generation, (b) scene-level generation, (c) generation acceleration, and (d) 4D generation. Images courtesy of [Kerbl et al., 2023, Tang et al., 2023, Ouyang et al., 2023, Zhou et al., 2023a, Yin et al., 2023].

6.1 Object-level 3D Generation

3D diffusion models provide good 3D consistency in 3D generation, while 2D diffusion models enjoy strong abilities of generalization. Combining the best of both worlds, Yi et al. [Yi et al., 2023] proposed GaussianDreamer for fast generation and real-time rendering. GaussianDreamer first initializes 3D Gaussians with the assistance of the 3D diffusion model to acquire geometry priors and introduces two operations of noisy point growing and color perturbation to supplement the initialized Gaussians for further content enrichment. Later, 3D Gaussians are optimized with the help of the 2D diffusion model and text prompts via the SDS. However, such a method still suffers from multi-face problems and fails to generate large-scale scenes.

Chen et al. [Chen et al., 2023d] proposed to guide the generation with the ordinary 2D SDS loss and an additional 3D point cloud diffusion prior to mitigating the Janus problem [Armandpour et al., 2023]. Specifically, this method first

initializes 3D Gaussians from customized shapes or the text-to-point-cloud diffusion model Point-E [Nichol et al., 2022] and then optimizes the representations with a combination of 2D and 3D SDS loss in the geometry optimization stage. In the appearance refinement stage, a compactness-based densification strategy is iteratively conducted to enhance geometry continuity and improve fidelity.

Xu et al. [Xu et al., 2024] revised the per-instance optimization setting in the traditional 3D generation with an amortized feed-forward pipeline called AGG, which can generalize to unseen objects of similar categories. AGG can reduce the need for test-time optimization by trading off the computation cost of the inference stage with the training stage. AGG takes a single image as input and decomposes the geometry and texture generation task into two distinct networks to produce 3D Gaussians at a low resolution. Subsequently, a UNet with point-voxel layers is employed to super-resolve the 3D Gaussian representation, improving its fidelity. However, such a practice also limits the number of Gaussians generated to represent very complex geometry.

The over-smoothing effect in SDS-based 3d generation methods has been identified. It has been revealed that the over-smoothing issue is mainly caused by the inconsistent and low-quality pseudo-GTs generated by the 2D diffusion models. Motivated by these observations, Liang et al. [Liang et al., 2023b] proposed a novel approach called Interval Score Matching (ISM) to counteract such deficiency. Specifically, DDIM inversion is introduced to increase the consistency of pseudo-GTs, making them more aligned with the inputs. Furthermore, to obtain pseudo-GTs with better visual quality, ISM chooses to conduct matching between two interval steps in the diffusion trajectory instead of matching the pseudo-GTs with images rendered by the 3D model.

6.2 Scene-level 3D Generation

Vilesov et al. [Vilesov et al., 2023] proposed CG3D to compositionally generate scalable 3D assets to form physically realistic scenes from text input only. CG3D represents each object in a scene with a set of Gaussian and converts objects into compositional coordinates with interaction parameters like rotation, translation, and scale.

Diffusion models trained on 3D scan datasets are inherently limited to generating domain-specific scenes due to the unrealistic nature of the training sets. LucidDreamer [Chung et al., 2023b] is proposed to create domain-free and high-quality 3D scenes from various types of inputs such as text, RGB and RGBD. With the help of Stable Diffusion [Rombach et al., 2022] and the estimated depth map, LucidDreamer first initializes the point cloud and then refines the point cloud through Dreaming and Alignment processes to form the SfM points for the optimization of Gaussian splats. The dreaming process creates new 3D points by completing partially projected images and lifting them into 3D space while the Alignment process seamlessly connects the new 3D points to the existing point cloud. Similarly, Text2Immersion [Ouyang et al., 2023] produces consistently immersive and photorealistic scenes from text prompts with a two-stage optimization of 3D Gaussians. In the first stage, an initial coarse Gaussian cloud is constructed incrementally, leveraging pre-trained 2D diffusion and depth estimation models under a set of anchor cameras rotated from the center view. Since the anchor cameras are selected only by rotation but not translation, a large portion of missing regions and noisy appearance may exist in the generated scene. Thus, the second stage focuses on 3D Gaussian refinement by incorporating additional views to fill in the missing areas and mitigate the issue of Gaussian noises.

6.3 3D Generation Acceleration

2D lifting methods with the NeRF representation [Poole et al., 2022] are notorious for their time-consuming optimization process. Therefore, Tang et al. [Tang et al., 2023] propose DreamGaussian to improve the 3D generation efficiency by replacing NeRF representation with 3D Gaussian Splatting. Specifically, DreamGaussian simplifies the optimization landscape with the progressive densification of Gaussian splatting, which initializes Gaussians with random positions and densifies them periodically to align with the generation progress. To enhance the generation quality, it further introduces an efficient mesh extraction algorithm with the block-wise local density query and a UV-space texture refinement stage that performs image space supervision. As a result, DreamGaussian can produce a high-quality textured mesh in just 2 minutes from a single-view image.

Despite the time efficiency advantage of text-to-3D methods utilizing 3D-GS over NeRF-based methods, they still experience prolonged generation time. This is primarily attributed to the intricate computations and extensive iterations involved in the gradient-based optimizations within the SDS or Variational Score Distillation (VSD) process. Zhou et al. presented Dreampropeller [Zhou et al., 2023a], a drop-in algorithm that utilizes parallel computation to expedite the distillation process by enabling faster ODE solving. The algorithm of Picard iterations [Alfuraidan and Ansari, 2016], as generalized by Dreampropeller, allows for the parallelization of sequential gradient update steps that involve variable dimension changes. This feature makes Dreampropeller well-suited for 3D methods utilizing 3D-GS, as the optimization process may involve varying numbers of Gaussians due to its split-and-prune operations. The experimental results demonstrate a 4.7-fold increase in speed with minimal impact on the quality of generation.

6.4 Text-to-4D Generation

Ling et al. [Ling et al., 2023] introduced Align Your Gaussians (AYG) to extend 3D synthesis to 4D generation with an additional temporal dimension. The 4D representation combines 3D Gaussian with deformation fields, which model scene dynamics of 3D Gaussians and transform the collection of them to represent object motion. AYG begins with generating an initial static 3D shape with a 3D-aware multi-view diffusion model and a regular text-to-image model. Then, a text-to-video model and a text-to-image model are used to optimize the deformation field to capture temporal dynamics and maintain high visual quality for all frames, respectively. Furthermore, a motion amplification mechanism as well as a new autoregressive synthesis scheme are adopted to generate and combine multiple 4D sequences for longer generations. Notably, due to the explicit nature of 3D Gaussians, different dynamic scenes, each with its own set of Gaussians and deformation field, can be combined, thereby enabling the composition of multiple 4D objects into large dynamic scenes. 4DGen [Yin et al., 2023] also leverages static 3D assets and monocular video sequences to conduct 4D generation. Both components can either be specified by users or generated by the multi-view diffusion model SyncDreamer [Liu et al., 2023a] and the video generation model. To guarantee consistency across frames, SyncDreamer is also used to construct point clouds from the anchor frames as 3D pseudo labels for scene deformation. 4DGen further adopts seamless consistency priors implemented with SDS and unsupervised smoothness regularizations.

NeRF-based 4D generation methods, like their counterparts in 3D domain, also experience long optimization time problems. DreamGaussian4D [Ren et al., 2023], a follow-up work of DreamGaussian [Tang et al., 2023], utilizes the explicit modeling of spatial transformations in Gaussian Splatting to simplify the optimization in image-to-4D generation. It first creates static 3D Gaussians from the input image using an enhanced variant of DreamGaussian called DreamGaussianHD. This variant pipeline aims to alleviate the blurriness problem in the original model. For the dynamic optimization, a driving video obtained from Stable Diffusion Video model is employed to optimize a time-dependent deformation field upon the static 3D Gaussians so as to learn the controllable and diverse motions. Finally, a video-to-video texture refinement strategy is adopted to enhance the quality of exported animated meshes.

To improve the efficiency in 4D generation domain, Pan et al. [Pan et al., 2024] propose Efficient4D, a fast video-to-4D object generation framework free of heavy supervision back-propagation through the large pre-trained diffusion model. To obtain labeled data for the training of 4D Gaussian Splatting, it utilizes an enhanced version of SyncDreamer to generate multi-view images of sampled frames in the input single-view video. Specifically, Efficient4D revises SyncDreamer with a time-synchronous spatial volume and a smoothing filter layer to impose temporal consistency across frames. During the reconstruction stage, this method optimizes 4D Gaussian representation using an inconsistency-aware loss function for coherent modeling of dynamics in both space and time.

Challenges: i) Compositional generation remains an open problem since most methods do not support such creation [Yin et al., 2023, Yi et al., 2023, Tang et al., 2023, Xu et al., 2024]. Even though CG3D [Vilesov et al., 2023] proposes a compositional framework, it supports only rigid-body interactions between objects. Besides, the compositional 4D sequences in AYG [Ling et al., 2023] fail to depict the topological changes of the dynamic objects. ii) It is non-trivial to adapt the adaptive density control operation in the original 3D-GS to the generation framework, so a plain approach [Xu et al., 2024] is to fix the number of Gaussians used to represent an object. However, such a design severely limits the model’s capability of creating complex geometry.

Opportunities: i) The multi-face problem, also known as Janus problem, exists in most 2D lifting methods [Tang et al., 2023, Vilesov et al., 2023]. As mentioned above, GaussianDreamer [Yi et al., 2023] manages to alleviate such deficiency by introducing 3D priors. In light of this, utilizing 3D-aware diffusion models or multi-view 2D diffusion models may be the possible direction for further improvement. ii) Personalized generation that takes various types of customized data as input and renders users more control over the generation process should be an exciting avenue for future work. iii) Text-to-3D methods tend to produce unsatisfying results when the textual prompt is comprised of ambiguous information and complicated logic. In this regard, enhancing the language understanding ability of the text encoder may also be able to boost the generation quality.

7 Perception

Leveraging 3D-GS, 3D perception has the potential to enhance open-vocabulary semantic object detection and localization (Fig. 7a), 3D segmentation (Fig. 7b), tracking of moving objects (Fig. 7c), and the development of Simultaneous Localization and Mapping (SLAM) systems (Fig. 7d).

7.1 Detection

The process of semantic object detection or localization in a 3D scene can significantly enhance environmental understanding and perception, as well as benefit applications such as autopilot systems and intelligent manufacturing.

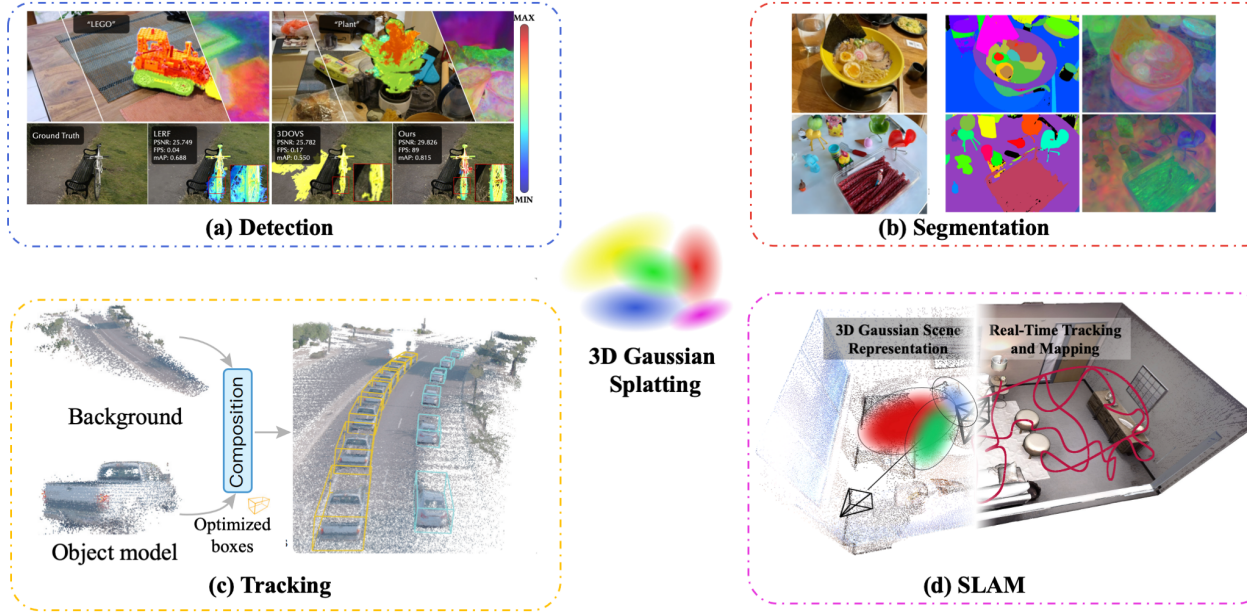


Figure 7: An illustration of 3D-GS on perception: (a) detection, (b) segmentation, (c) tracking, and (d) SLAM. Images courtesy of [Zhou et al., 2023b, Shi et al., 2023, Ye et al., 2023, Yan et al., 2024].

Encouraged by the success of ChatGPT, Shi et al. [Shi et al., 2023] introduced Language Embedded 3D Gaussians, a scene representation specifically crafted for open-vocabulary query tasks, which successfully incorporates quantized compact semantic features onto extensive 3D Gaussians, minimizing memory and storage requirements. In order to mitigate semantic inconsistencies arising from varying perspectives, a feature smoothing procedure is proposed to dynamically reduce the spatial frequency of embedded semantic features, leveraging spatial position and semantic uncertainty of 3D Gaussians. At the same time, Zuo et al. [Zuo et al., 2024] proposed Foundation Model Embedded Gaussian Splatting (FMGS), which integrates 3D-GS for the representation of geometry and appearance, along with Multi-Resolution Hash Encodings (MHE) for efficient language embedding. FMGS aims to tackle memory limitations in room-scale scenes. Moreover, to tackle the issue of pixel misalignment, FMGS incorporates a pixel alignment loss to align the rendered feature distance of identical semantic entities with pixel-level semantic boundaries. The results of FMGS exhibit significant multi-view semantic consistency and impressive performance in localizing semantic objects within an open-vocabulary context.

7.2 Segmentation

The significance of 3D scene segmentation lies not only in improving the accuracy of scene segmentation but also in providing robust support for real-world 3D perception tasks. The applications of 3D scene segmentation methods, ranging from real-time scene editing and object removal to object inpainting and scene recomposition, have undoubtedly broadened the horizons of computer vision in domains including virtual reality and autonomous driving.

The incorporation of a 2D segmentation model can be a valuable asset in guiding the segmentation process of 3D-GS. This intuitive concept has the potential to improve both the accuracy and efficiency of the segmentation procedure. Lan et al. [Lan et al., 2023] introduced a 3D Gaussian segmentation method that utilizes 2D segmentation as supervision, where each 3D Gaussian is assigned an object code to represent its categorical probability distribution. Guidance is provided to ensure the accurate classification of each 3D Gaussian by minimizing the discrepancy between the 2D segmentation map and the rendered segmentation map at a specific pose. Moreover, KNN clustering is employed to tackle the issue of semantic ambiguity within 3D Gaussians, while statistical filtering is implemented to eliminate incorrectly segmented 3D Gaussians. This approach successfully acquires the semantic knowledge of a 3D scene and efficiently segments multiple objects from a specific viewpoint within a brief timeframe, yielding compelling outcomes.

Moreover, several approaches draw inspiration from 2D visual foundation models [Kirillov et al., 2023, Liu et al., 2023b] to leverage their robust zero-shot segmentation capabilities for guiding the segmentation of 3D-GS. By employing these methods, researchers can harness the advantageous features of the 2D model to improve the accuracy and effectiveness of the segmentation process in the 3D domain. Ye et al. [Ye et al., 2023] introduced Gaussian Grouping for simultaneous reconstruction and segmentation of diverse elements within open-world 3D scenes. The proposal includes an Identity Encoding for 3D Gaussians, supervised by both 2D mask predictions from SAM and 3D spatial consistency, which enables each Gaussian to be associated with its represented instances or elements in the 3D scene. Leveraging this discrete and grouped 3D scene representation, Gaussian Grouping showcases its ability to support various scene editing applications, encompassing 3D object removal, object inpainting, and scene recomposition. Gaussian Grouping achieves a high-quality visual effect while maintaining efficient processing time. Meanwhile, Cen et al. [Cen et al., 2023] presented the Segment Any 3D Gaussians (SAGA) to integrate a 2D segmentation foundation model with 3D-GS for 3D interactive segmentation. SAGA incorporates multi-granularity 2D segmentation results from the foundation model into 3D Gaussian point features, eliminating the requirement for the time-consuming multiple forwarding of the 2D segmentation model during inference. SAGA trains 3D features for Gaussians based on automatically extracted masks, and a set of queries is generated with input prompts, efficiently retrieving the expected Gaussians through feature matching. Furthermore, SAGA facilitates multi-granularity segmentation and accommodates various prompts, including points, scribbles, and 2D masks. Also inspired by 2D foundation models, Zhou et al. [Zhou et al., 2023b] proposed Feature-3DGS, a feature field distillation technique based on 3D-GS for 3D scene understanding and interaction tasks. Feature-3DGS initially acquires a semantic feature from each 3D Gaussian, in addition to the color information. By utilizing differentiable splatting and rasterization techniques on the feature vectors, Feature-3DGS facilitates the extraction of the feature field while being guided by 2D foundation models. Furthermore, Feature-3DGS acquires knowledge of a well-organized, lower-dimensional feature field. This field is subsequently enhanced through the utilization of a streamlined convolutional decoder during the final stages of the rasterization process. Feature-3DGS facilitates complex semantic tasks such as editing, segmentation, and language-prompted interactions.

Hu et al. [Hu et al., 2024] proposed a SA-GS for segmenting objects in 3D Gaussians. Notably, SA-GS does not require any training process or learnable parameters. The segmentation obtained using SA-GS enables efficient collision detection and scene editing, including tasks such as object removal, translation, and rotation within 3D scenes.

7.3 Tracking

As discussed in Sec. 4, utilization of 3D-GS facilitates the reconstruction of dynamic scenes. Consequently, the tracking of dynamic objects within these scenes has emerged as a novel area of exploration, contributing significantly to applications such as autonomous driving.

Zhou et al. [Zhou et al., 2023c] introduced DrivingGaussian for reconstructing dynamic large-scale driving scenes. DrivingGaussian progressively models the static background by utilizing incremental static 3D Gaussians in scenes that contain moving objects. DrivingGaussian utilizes a composite dynamic Gaussian graph to accurately reconstruct individual objects, restore their positions, and effectively handle occlusion relationships in the presence of multiple moving objects. Moreover, the utilization of LiDAR prior to 3D-GS facilitates the improvement of scene reconstruction by capturing finer details and ensuring the preservation of panoramic consistency. DrivingGaussian successfully achieves high-fidelity and multi-camera consistent photorealistic surround-view synthesis, making it applicable for a wide range of tasks, including the simulation of corner cases.

At the same time, Yan et al. [Yan et al., 2024] introduced StreetGaussian for modeling dynamic urban street scenes from monocular videos. StreetGaussian represents the dynamic urban street as a collection of point clouds that are augmented with semantic logits and 3D Gaussians. These components are assigned to either foreground vehicles or the background. To accurately represent the movement of foreground object vehicles, we optimize each object’s point cloud by incorporating trackable poses and a dynamic spherical harmonics model to account for their dynamic appearance. Despite its ability to facilitate the seamless creation of object vehicles and backgrounds for scene editing operations, as well as its capability to achieve high-speed rendering, this approach does have certain limitations. Specifically, StreetGaussian is limited to reconstructing rigid dynamic scenes, such as stationary streets with only moving vehicles, and is incapable of handling non-rigid dynamic objects, such as pedestrians in motion.

Since tracking the movement of small objects can be challenging, Cotton et al. [Cotton and Peyton, 2024] applied dynamic Gaussian splatting [Luiten et al., 2023] with depth supervision to analyze sparse, markerless motion capture data, specifically focusing on the accurate assessment of movement in infants and neonates. This approach employs semantic segmentation masks to enhance the emphasis on the infant, thereby resulting in improved scene initialization. Additionally, an alternative dynamic tracking method using deformation fields was implemented based on [Yang et al., 2023b]. This method models the changes in location, rotation, and scale by considering the initial 3D locations and the

desired time point. This approach has illustrated its ability to produce innovative viewpoints of scenes and track the movements of infants.

7.4 Simultaneous Localization and Mapping

In the realm of 3D perception, the integration of 3D-GS into Simultaneous Localization and Mapping (SLAM) systems has garnered significant attention. In this section, we will explore the diverse applications and advancements in SLAM, which are made possible by integrating the 3D Gaussian representation. Furthermore, this section underscores the efficacy of current methodologies in addressing real-world scenarios and highlights the continuous growth of possibilities within the SLAM domain.

Due to the significance of efficiency, Yan et al. [Yan et al., 2023b] presented GS-SLAM to integrate 3D Gaussian representation into the SLAM system. GS-SLAM utilizes a real-time differentiable splatting rendering pipeline, resulting in notable enhancements in map optimization and RGB-D re-rendering speed. GS-SLAM introduces an adaptive strategy for expanding 3D Gaussians, aiming to efficiently reconstruct newly observed scene geometry. Furthermore, it employs a coarse-to-fine technique to select reliable 3D Gaussians, enhancing the accuracy of camera pose estimation. GS-SLAM effectively improves the trade-off between efficiency and accuracy, surpassing recent SLAM methods that utilize neural implicit representations. Meanwhile, Matsuki et al. [Matsuki et al., 2023] introduced a real-time SLAM system which leverages 3D-GS for incremental 3D reconstruction. This approach is applicable to both moving monocular and RGB-D cameras, enabling near real-time performance. The proposed method formulates camera tracking for 3D-GS through direct optimization against the 3D Gaussians, facilitating fast and robust tracking with a broad basin of convergence. Leveraging the explicit nature of the Gaussians, the method introduces geometric verification and regularization to handle ambiguities in incremental 3D dense reconstruction. Notably, this method achieves great results in novel view synthesis, trajectory estimation, and the reconstruction of tiny and even transparent objects. Moreover, Huang et al. [Huang et al., 2023b] proposed Photo-SLAM to introduce a hyper primitives map by integrating both explicit geometric features for localization and implicit photometric features for representing texture information. Notably, Photo-SLAM incorporates Gaussian-Pyramid-based learning to efficiently capture multi-level features, thereby enhancing the photorealistic quality of the mapping process. The efficacy of Photo-SLAM in online photorealistic mapping is demonstrated, showcasing its potential for applications in advanced robotics in real-world scenarios.

To effectively utilize monocular input data from SLAM, it is crucial to design meticulous methods that incorporate 3D-GS. For example, Keetha et al. [Keetha et al., 2023] presented SplaTAM to leverage 3D-GS for dense SLAM using a single unposed monocular RGB-D camera. SplaTAM commences by estimating the camera pose for a novel image through silhouette-guided differentiable rendering. Subsequently, SplaTAM dynamically increases map capacity by incorporating new Gaussians derived from the rendered silhouette and input depth information. Finally, it updates the underlying Gaussian map using differentiable rendering. SplaTAM allows for explicit knowledge of map spatial extent and facilitates streamlined map densification, addressing the shortcomings observed in previous representations based on radiance fields. Yugay et al. [Yugay et al., 2023] presented a SLAM method that utilizes 3D-GS as the scene representation. This approach introduces strategies for initializing and optimizing Gaussian splats, thereby extending their application from offline multiview scenarios to sequential monocular RGB-D input data setups. Additionally, an extension of Gaussian splitting has been developed to enhance the encoding of geometry, enabling reconstruction beyond radiance fields in a monocular setup. This proposed representation greatly facilitates interactive-time reconstruction and photo-realistic rendering.

7.5 Camera Pose Estimation

Camera pose estimation stands as a foundational aspect in the realms of 3D reconstruction and perception. The incorporation of 3D-GS has the potential to provide insightful approaches to this essential topic.

In SLAM, the task of estimating the 6D pose poses a considerable challenge. To solve this challenge, Sun et al. [Sun et al., 2023] introduced iComMa by integrating traditional geometric matching methods with rendering comparison techniques. iComMa inverts the 3D-GS to capture pose gradient information for precise pose computation and adopts a render-and-compare strategy to ensure increased accuracy during the final phase of optimization. Additionally, a matching module is incorporated to enhance the model’s robustness against unfavorable initializations via minimizing distances between 2D keypoints. iComMa is designed to effectively handle a wide range of complex and challenging scenarios, including cases with significant angular deviations while maintaining a high level of accuracy in predicting outcomes.

Challenges: (i) The existing tracking methods for dynamic scene objects based on 3D-GS may encounter challenges in tracking deformable objects, such as pedestrians, posing difficulties for systems like autonomous driving. (ii) Moreover,

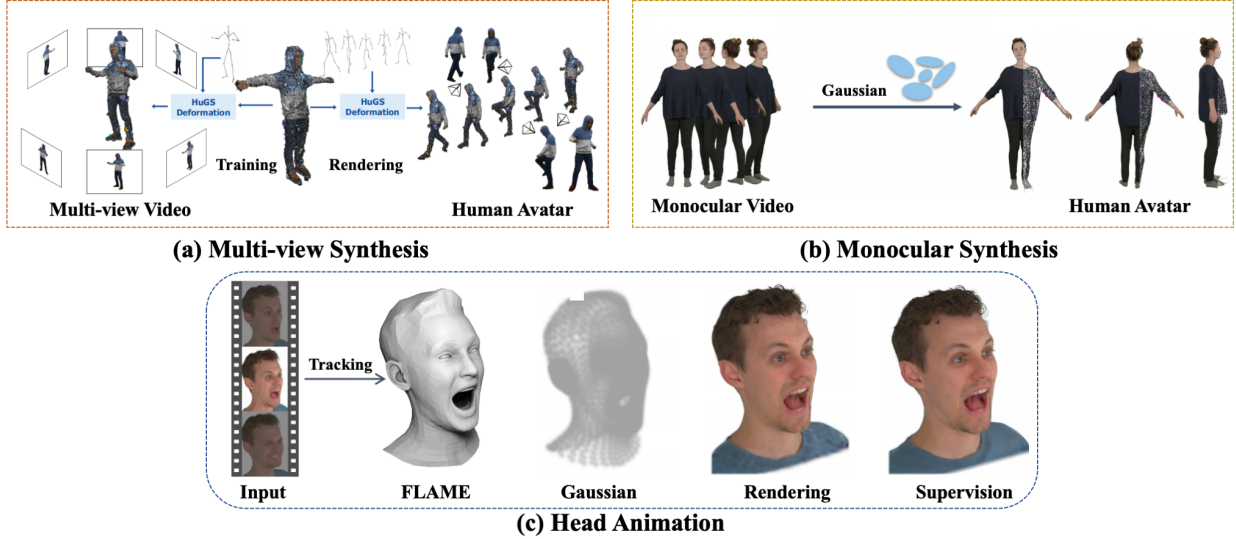


Figure 8: An illustration of 3D-GS on human avatar animation: (a) multi-view synthesis, (b) monocular synthesis, and (c) head animation. Images courtesy of [Moreau et al., 2023, Li et al., 2024, Qian et al., 2023a].

the detection of highly reflective or translucent objects, such as televisions and mirrors, remains a challenging task as the modeling capabilities of 3D-GS for these objects are limited. (iii) A SLAM system might exhibit sensitivity to various factors, including motion blur, substantial depth noise, and aggressive rotation. (vi) Moreover, in the representation of 3D-GS, a Gaussian distribution can be linked to multiple objects, thereby increasing the complexity of accurately segmenting individual objects utilizing feature matching.

Opportunities: (i) Real-time tracking based on 3D-GS has the potential to be applied in various medical scenarios, including radiation therapy. (ii) Besides, inputting known camera intrinsics and dense depth is essential for executing SLAM, and eliminating these dependencies presents an intriguing direction for future exploration.

8 Virtual Humans

Learning virtual human avatars with implicit neural representations like NeRF and SDF suffers from long optimization and rendering time and struggles to generate satisfactory-quality novel body poses. In contrast, utilizing the 3D Gaussian representation is experimentally demonstrated to improve training and rendering speeds and offer explicit control of human body deformation. Also, forward skinning in 3D Gaussian methods avoids the correspondence ambiguities that are present in inverse skinning used in neural implicit representations [Jena et al., 2023].

Typically, 3D Gaussian-based methods start with initializing Gaussians with an SMPL template and then deform the representations into the observation space using Linear Blend Skinning (LBS). Gaussians are then rendered and supervised by either multi-view (Fig. 8a) or monocular videos (Fig. 8b). Besides, some methods specialize in reconstructing human head avatars (Fig. 8c), while some focus on the generalizable pipeline instead of per-subject optimization.

8.1 Multi-view Video Synthesis

Moreau et al. [Moreau et al., 2023] proposed a HuGS to render photo-realistic human body avatars from multi-view videos with an animatable human body, which represents the human body with a set of 3D Gaussians. 3D Gaussians in HuGS build upon the original setting with the addition of a skinning weight vector that regulates the influence of each body joint on how the Gaussian moves and a latent code that encodes the non-rigid motion. HuGS applies LBS to deform the canonical primitives initialized by the SMPL model and learns only the skinning weights. Since LBS only encodes the rigid deformations of the body joints, HuGS subsequently introduces a local non-rigid refinement stage to model the non-rigid deformation of the garments, considering both the body pose encoding and ambient occlusions. Though achieving competitive performance on novel pose synthesis, HuGS optimizes and deforms each Gaussian independently, ignoring the intrinsic relation between Gaussians in local neighborhoods. Based on the observation that explicit point-based representations have the potential to be parameterized on 2D maps, Li et al. [Li et al., 2023a]

facilitated Gaussian-based modeling with powerful 2D CNNs to faithfully reconstruct higher-fidelity avatars. After obtaining the character-specific template from multi-view images and diffusing into it the skinning weights of SMPL, this method predicts two pose-dependent canonical Gaussian maps in the UV space through the StyleUNet [Wang et al., 2023a]. Specifically, given a training pose, the template is first deformed to the posed space via LBS, and two position maps are produced by orthogonally projecting the posed template to the front and back views. Subsequently, Gaussian maps are generated with position maps serving as the pose condition, and thus canonical Gaussians are extracted from each pixel. Moreover, for the generalization to novel poses, PCA is utilized to project a novel driving pose signal into the distribution of seen training poses. ASH [Pang et al., 2023] also attaches Gaussian splats to the deformable character model [Habermann et al., 2021] and parameterizes them in 2D texture space, with each texel covered by a triangle representing a Gaussian. Besides, a 2D geometry decoder and a 2D appearance decoder are adopted to separately predict the shape-related parameters and the Spherical Harmonics. Subsequently, Gaussian splats from the canonical position are transformed to the posed space through Dual Quaternion skinning [Kavan et al., 2007] and supervised solely on the multi-view videos.

Departing from the commonly used LBS, D3GA [Zielonka et al., 2023] employs cage deformation, a classic volumetric deformation method to transform Gaussians to represent drivable human avatars. Notably, the deformation is conducted in a compositional manner where the body, face, and garment avatar are deformed by separate cages and each part is controlled by three specialized MLPs, the cage node correction network, the Gaussian correction network, and the shading network.

HiFi4G [Jiang et al., 2023c] resorts to traditional non-rigid tracking for high-fidelity human performance rendering from multi-view videos. A dual-graph mechanism, which consists of a coarse deformation graph and a fine-grained Gaussian graph, is first introduced to bridge 3D Gaussian with non-rigid tracking. The former first generates per-frame geometry proxies using NeuS2 [Wang et al., 2023b] and then applies the Embedded Deformation (ED) [Sumner et al., 2007] to establish model-to-model motion correspondences. Then, the fine-grained Gaussian graph is generated by initializing Gaussians from the mesh of the first frame and applying pruning and densification operations to the subsequent keyframes for temporal coherence. In the optimization step, HiFi4G employs ED graph to warp Gaussian under the constraint of a temporal regularizer, a smooth term, and an adaptive weighting mechanism.

8.2 Monocular Video Synthesis

Concurrently, Kocabas et al. [Kocabas et al., 2023] designed a deformation model to represent the animatable human and the static scene with 3D Gaussians from only a monocular video. In practice, the human body and the scene are disentangled and separately constructed from the SMPL body model the structure-from-motion point cloud. The human Gaussians are parameterized by their center locations in a canonical space, a feature triplane and three MLPs which predict properties of the Gaussians and are further optimized in a similar pipeline to [Moreau et al., 2023]. Similar to [Kocabas et al., 2023], ParDy-Human [Jung et al., 2023] separates the human and the background with two sets of Gaussians. Additionally, the human Gaussian representation is extended with two extra features, parent index and surface normal, indicating the mesh face that the Gaussian is generated from. Thus, the canonical Gaussian can be deformed to the pose with Per Vertex Deformation (PVD) according to its parent mesh face. The garment motions are further refined by a deformation refinement that predicts residual refinements for PVD deformations. Besides, the surface normal is updated through the deformations to obtain a more realistic direction for calculating Spherical Harmonics. Li et al. [Li et al., 2023b] proposed Human101 for both fast reconstruction and real-time rendering from monocular videos. For fast convergence, Human101 first extracts the point cloud from four frames covering the front, back, left and right views of the human body and then converts the generated point cloud into canonical Gaussians. In the deformation process, Human101 assigns each Gaussian to its nearest SMPL triangular facet and deforms its rotation and spherical harmonics with Triangular Face Rotation accordingly.

3DGS-Avatar [Qian et al., 2023b] also initializes a set of canonical Gaussians via sampling on the SMPL mesh template. Following [Weng et al., 2022], it decomposes the human deformation into a non-rigid part that encodes pose-dependent cloth deformation, and a rigid transformation controlled by the human skeleton. Since the view-dependent color encoding does not suit the monocular setting, 3DGS-Avatar substitutes the convention of learning spherical harmonic coefficients with a color MLP. In practice, it canonicalizes the viewing direction used in the color modeling and additionally learns a per-frame latent code to encode the different light effects across frames.

Instead of optimizing per-Gaussian colors, Jena et al. [Jena et al., 2023] proposed a novel neural color field to implicitly regularize the color of nearby Gaussians, which later provides an additional 3D supervision to the Gaussian positions. The visualized results prove that this operation effectively reduces the texture artifacts on test frames.

To circumvent the inaccurate motion estimation in the monocular setting, Hu et al. [Hu et al., 2023] proposed GaussianAvatar to jointly optimize motion and appearance with isotropic 3D Gaussians. Specifically, given a fitted

SMPL model, the network encodes the pose-dependent feature from a 2D UV position map and further integrates the feature with an optimizable feature tensor that encodes the coarse global appearance. Thus, the integrated feature serves as the input for the Gaussian parameter encoder to predict the Gaussian properties like position offset, color and scale. Notably, the human avatar is represented by isotropic Gaussians with fixed rotation and opacity since anisotropic 3D Gaussians are prone to overfitting the most frequently seen view via monocular supervisions, resulting in poorer performance in unseen areas.

The direct application of LBS transformation for 3D Gaussians may introduce inaccurate information derived from SMPL. In this regard, GauHuamn [Hu and Liu, 2023] starts with LBS weights from SMPL and rectifies SMPL poses with an effective pose refinement module. GauHuamn also integrates the KL divergence of 3D Gaussians to regulate the split and clone process, taking the crucial metric, the distance between 3D Gaussians, into consideration. To speed up the optimization, a novel merge operation is introduced to merge redundant Gaussians that meet certain criteria. The inaccurate mapping from the canonical space to the observation space may induce overfitting and artifacts. To tackle this, Li et al. [Li et al., 2024] proposed to preserve the local geometry property of 3D Gaussians during the deformation with three regularization losses, i.e., the local-rigidity loss, the local-rotation loss, and the local-isometry loss [Luiten et al., 2023]. Since the monocular video input inherently lacks multi-view supervision, a split-with-scale operation to address the potential blurries and oversized Gaussians and a pose refinement to optimize the SMPL pose parameters during training are introduced for further refinement.

8.3 Human Head Animation

GaussianAvatars [Qian et al., 2023a] focuses on the reconstruction of head avatars by rigging 3D Gaussians to a parametric morphable face model. In particular, 3D Gaussians are initialized at the center of each triangle of the FLAME [Li et al., 2017] mesh, with their parameters defined by the triangle properties. Besides, to accommodate the adaptive density control operations to the method without breaking the connection between triangles and splats, a binding inheritance strategy is designed to additionally parameterize the Gaussian with the index of its parent triangle so that new Gaussian points remain rigged to the FLAME mesh. However, such a method lacks control over areas that are not modeled by FLAME such as hair and other accessories. Dhano et al. [Dhano et al., 2023] proposed a head animation method called HeadGas that can work with different 3D morphable models from monocular video inputs. To create the correspondence between the specific expression and 3D Gaussians, this method extends Gaussian representation with a base of latent features, which is multiplied with an expression vector and then fed to the MLP to yield the final color and opacity. Since 3D Morphable Model (3DMM) based methods often fail to model non-facial structures such as eyeglasses and hairstyles, Zhao et al. [Zhao et al., 2024] proposed a Point-based Morphable Shape Model (PMSM), which replaces meshed with points for enhanced representation flexibility. To be concrete, PMSM builds on FLAME to inherit its morphable capability. Then, it converts the FLAME mesh to points by uniformly sampling points on the surface of the mesh. Additionally, points off the meshes are sampled to capture complex structures ignored by the FLAME model. For faster convergence of head shape alignment, the process is conducted in an analysis-by-synthesis manner with point splatting instead of Gaussian splitting. Finally, 3D Gaussian is employed in combination with PMSM for effective fine-detail rendering.

Chen et al. [Chen et al., 2023e] adopted a different approach to deform the Gaussian representation from monocular videos by transforming the mean position of Gaussians from the canonical space to the deformed space with LBS and adjusting other Gaussian parameters correspondingly with a deformation field. Similarly, Xu et al. [Xu et al., 2023a] proposed a fully learnable expression-conditioned deformation field to avoid the limited capability of the LBS-based formulation. Specifically, this method inputs the positions of the 3D Gaussians with expression coefficients into an MLP to directly predict the displacements from the neutral expression to the target one. Besides, instead of initializing Gaussians with a morphable template, it designs a geometry-guided initialization strategy by optimizing an SDF field, a color field and a deformation field to extract a mesh and construct Gaussians on the basic head surface. GaussianHead [Wang et al., 2023c] disentangles the modeling of the head geometry and texture attributes by utilizing a motion deformation field to fit the head shape as well as dynamic facial movements and a multi-resolution tri-plane to store the appearance information of Gaussians. To resolve the feature dilution problem, this monocular-video-based method devises a novel Gaussian derivation strategy, which generates multiple doppelgangers of each core Gaussian in the canonical space through learnable rotation transformations and then integrates sub-features of these doppelgangers to form the final canonical feature for the core Gaussian.

8.4 Generalizable Methods

Contrary to most methods relying on per-subject optimization, Zheng et al. [Zheng et al., 2023] presented a generalizable 3D-GS to synthesize novel views of unseen human performers in real time without any fine-tuning or optimization. The proposed GPS-Gaussian directly regresses Gaussian parameters in a feed-forward manner from massive 3D human scan

data with diverse properties to learn abundant human priors, thus enabling instantaneous human appearance rendering. Moreover, GPS-Gaussian adopts the efficient 2D CNN to encode the source view image and predict the 2D Gaussian parameter maps. Specifically, the learned depth map via the depth estimation module and the RGB image serve as the 3D position map and the color map, respectively, to formulate the Gaussian representation while the other parameters of 3D Gaussians are predicted in a pixel-wise manner. Later, these parameter maps are unprojected to 3D space and aggregated for novel view rendering.

Challenges: i) The garment deformation is not well learned in 3D Gaussian human body initialized by the SMPL model and LBS, e.g., ParDy-Human [Jung et al., 2023] tends to produce artifacts in the uni-colored garments with large deformations [Moreau et al., 2023] points out that the modeling of loose garments may be improved by incorporating more physics priors. ii) The environment lighting is not parameterized in most methods, which makes relighting the avatars infeasible. iii) Though much progress has been made in reconstructing human avatars from monocular videos, it is still a tricky problem to recover the fine details since only limited information is provided from the sparse view. iv) Currently, 3D Gaussians in most methods are optimized and deformed independently, ignoring the intrinsic structure and connectivity relation between Gaussians in local regions.

Opportunities: i) For human head modeling, methods that utilize 3DMM to control the motions also fail to express subtle facial expressions. Exploring a more effective method to separately control the non-rigid deformation is a focus of future work. ii) How to extract meshes from learned 3D Gaussians remains a future work to be investigated. iii) The reconstruction performance of both the 3DMM-based methods and SMPL-based methods is constrained by the initialization of model parameters. The inaccuracy in the fixed parameters may severely affect the model’s alignment with the supervisions, thus leading to blurred texture. Noted that 3DMM and SMPL fail to model the loose structure of the human body. In this regard, enhancing the expression ability of the template model during the optimization is a promising breakthrough in future work.

9 Discussions and Future Work

3D Gaussian Splatting has demonstrated significant potential in the fields of computer graphics and computer vision. Nevertheless, various challenges persist due to the intricate structures and diverse tasks associated with 3D Gaussian Splatting. This section aims to address these challenges and present potential avenues for future research.

Handling Floating Elements in 3D-GS. A notable issue in 3D Gaussian Splatting is the prevalence of floating elements within the rendered space, primarily originating from image backgrounds. Employing opacity thresholds has been suggested to reduce the occurrence of these floats, enhancing image rendering quality as measured by PSNR and SSIM metrics [Fan et al., 2023]. However, these floating elements significantly impact the visual quality of the rendered images. A potential area of research could focus on strategies to anchor these floats closer to surfaces, thereby enhancing their positional relevance and contribution to image quality.

Trade-off Between Rendering and Reconstruction. The presence of floating elements, as previously mentioned, significantly influences the visual quality of images. However, their impact extends beyond rendering to affect mesh reconstruction processes. The SuGaR method [Guédon and Lepetit, 2023] utilizes an opacity-based approach to generate 3D Gaussians around the mesh surface, which, while beneficial for reconstruction, can compromise rendering quality. This highlights the need for a nuanced approach to balance rendering excellence with accurate reconstruction. Exploring how 3D-GS could enhance or complement other advanced multi-view reconstruction techniques represents another promising research avenue [Chen et al., 2023a].

Rendering Realness. Current lighting decomposition methods show limited effectiveness in scenes with indistinct boundaries, often requiring the inclusion of object masks during optimization. This limitation primarily arises from the detrimental influence of the background on the optimization process, a consequence of the distinctive qualities of the point clouds generated through 3D Gaussian Splatting. Unlike conventional surface points, these point clouds display particle-like properties, including color and partial transparency, deviating from conventional surface points. Considering these challenges, integrating Multi-View Stereo (MVS) into the optimization process emerges as a promising direction. Such integration could significantly improve geometry accuracy, presenting a promising avenue for future research.

Real-time Rendering. To facilitate real-time rendering, Scaffold-GS [Lu et al., 2023] introduces anchor points from a sparse voxel grid [Xu et al., 2023b], which aids in distributing local 3D Gaussians and thus improves rendering speed. However, the method’s reliance on a uniform grid size limits its adaptability. The use of octree representations emerges as a promising alternative, offering the flexibility to divide more complex regions into smaller grids for detailed processing. While these methods show potential for achieving real-time rendering in small scenes, scaling up to large environments, such as cityscapes [Xu et al., 2023b], will require further innovation and additional efforts.

Few-shot 3D-GS. Recent few-shot studies [Zhu et al., 2023, Chung et al., 2023a] explore optimizing Gaussian splatting with depth guidance in a few-shot setting. While promising, these approaches face notable challenges. The success of few-shot methods heavily relies on the accuracy of monocular depth estimation models. Moreover, their performance may vary across different data domains, affecting the optimization process for 3D-GS. Additionally, the dependency on fitting the estimated depth to COLMAP [Schonberger and Frahm, 2016] points introduces reliance on the performance of COLMAP itself. Consequently, these limitations pose challenges in handling textureless areas or complex surfaces where COLMAP [Schonberger and Frahm, 2016] may encounter difficulties. For future research, it would be beneficial to investigate the optimization of 3D scenes using interdependent depth estimates, reducing reliance on COLMAP points. Another avenue for future work involves investigating methods to regularize geometry across diverse datasets, particularly in areas where depth estimation, such as the sky, presents challenges.

Integration of Physics. In contrast to the natural world, where the physical behavior and visual appearance of materials are inherently interconnected, the traditional physics-based visual content generation pipeline has been a laborious and multi-stage process. This process involves constructing the geometry, preparing it for simulation (often using techniques like tetrahedralization), simulating the physics, and eventually rendering the scene. Although this sequence is effective, it introduces intermediate stages that can result in discrepancies between the simulation and the final visualization. This disparity is also evident within the NeRF paradigm [Li et al., 2023c, Chu et al., 2022], where the rendering geometry is embedded within a simulation geometry. To address this issue, it is recommended to unite these two aspects by advocating for a unified representation of material substance that can be utilized for both simulation and rendering purposes. Furthermore, a promising direction is the automatic assignment of materials to 3D-GS.

Accurate Reconstruction. The original 3D-GS cannot distinguish between specular and non-specular areas. Therefore, 3D-GS will produce unreasonable 3D Gaussians in the specularly reflected parts [Jiang et al., 2023a, Gao et al., 2023]. The presence of irrational 3D Gaussians can significantly influence the reconstruction process, leading to the generation of flawed meshes. Furthermore, it has been observed that the inclusion of specular reflection components can also result in the production of unreliable meshes [Guédon and Lepetit, 2023]. Hence, in order to achieve precise reconstruction, it is essential to decompose the 3D Gaussian through illumination prior to accurately reconstructing the mesh.

Realistic Generation. Pioneered by DreamGaussian [Tang et al., 2023], GaussianDreamer [Yi et al., 2023], 3D-GS begins its journey on 3D generation. However, the geometries and textures of the generated 3D assets still require improvement. In terms of geometries, the integration of more precise SDF and UDF into the 3D-GS allows for the generation of meshes that are more realistic and accurate. Additionally, various conventional graphic techniques, such as Medial Fields [Rebain et al., 2021], can be effectively utilized. Regarding textures, two recently proposed methods, MVD [Liu et al., 2023c] and TexFusion [Cao et al., 2023], demonstrate impressive capabilities in texture generation. These advancements have the potential to be applied in the context of textured mesh generation with 3D-GS. Additionally, Relightable3DGaussian [Gao et al., 2023] and GaussianShader [Jiang et al., 2023a] have explored the shading aspects of 3D-GS. However, the question of BRDF decomposition on the generated meshes remains unanswered.

Expanding 3D-GS with Large Foundation Models. Recent studies, such as Shi et al. [Shi et al., 2023], have demonstrated that embedding language into 3D-GS can significantly enhance 3D scene understanding. With the advent of large foundation models in 2023, their remarkable capabilities have been showcased across a broad spectrum of vision tasks. Notably, the SAM model has emerged as a powerful tool for segmentation, finding successfully application within the 3D-GS [Ye et al., 2023, Zhou et al., 2023b, Cen et al., 2023]. Beyond segmentation, LLM models have shown promise for language-guided generation, manipulation, and perception tasks. This highlights the versatility and utility of these models in a wide range of applications, further emphasizing their significance in 3D-GS. Recent studies, such as Shi et al. [Shi et al., 2023], have demonstrated that embedding language into 3D-GS can significantly enhance 3D scene understanding. With the advent of large foundation models in 2023, their remarkable capabilities have been showcased across a broad spectrum of vision tasks. Notably, the SAM model has emerged as a powerful tool for segmentation, finding successful application within the 3D-GS [Ye et al., 2023, Zhou et al., 2023b, Cen et al., 2023]. Beyond segmentation, LLM models have shown promise for language-guided generation, manipulation, and perception tasks. This highlights the versatility and utility of these models in a wide range of applications, further emphasizing their significance in 3D-GS.

Taming 3D-GS for Other Methods. Several works employ 3D-GS as a supplementary tool to improve performance. For instance, NeuSG [Chen et al., 2023a] utilizes 3D-GS to enhance the reconstruction of NeuS, while SpecNerf [Ma et al., 2023] incorporates Gaussian directional encoding to model specular reflections. Consequently, the distinctive characteristics of 3D-GS can be seamlessly integrated into existing methods to further boost their performance. It is conceivable that 3D-GS can be combined with the Large Reconstruction Model (LRM) [Xu et al., 2023c], or with existing perception techniques in the field of Autonomous Vehicles, to enhance their perception capabilities.

10 Conclusions

This paper offers a comprehensive and up-to-date overview of 3D Gaussian Splatting, summarizing existing methods and their applications. We begin by reviewing papers focused on optimizing 3D-GS for efficiency, realism, cost, and physics. Subsequently, we systematically explore the five main applications of 3D-GS, including reconstruction, manipulation, generation, perception, and human-centric applications. Lastly, we delve into challenges and potential future directions in this field. Additionally, we provide a comparative summary of methods, serving as a valuable resource for researchers in 3D vision and computer graphics.

References

- Bernhard Kerbl, Georgios Kopanas, Thomas Leimkühler, and George Drettakis. 3d gaussian splatting for real-time radiance field rendering. *ACM TOG*, 42(4), 2023.
- Tao Lu, Mulin Yu, Linning Xu, Yuanbo Xiangli, Limin Wang, Dahua Lin, and Bo Dai. Scaffold-gs: Structured 3d gaussians for view-adaptive rendering. *arXiv:2312.00109*, 2023.
- Zehao Yu, Anpei Chen, Binbin Huang, Torsten Sattler, and Andreas Geiger. Mip-splatting: Alias-free 3d gaussian splatting. *arXiv:2311.16493*, 2023a.
- Guanjun Wu, Taoran Yi, Jiemin Fang, Lingxi Xie, Xiaopeng Zhang, Wei Wei, Wenyu Liu, Qi Tian, and Xinggang Wang. 4d gaussian splatting for real-time dynamic scene rendering. *arXiv:2310.08528*, 2023a.
- R James Cotton and Colleen Peyton. Dynamic gaussian splatting from markerless motion capture reconstruct infants movements. In *WACV*, pages 60–68, 2024.
- Antoine Guédon and Vincent Lepetit. Sugar: Surface-aligned gaussian splatting for efficient 3d mesh reconstruction and high-quality mesh rendering. *arXiv:2311.12775*, 2023.
- Jaeyoung Chung, Jeongtaek Oh, and Kyoung Mu Lee. Depth-regularized optimization for 3d gaussian splatting in few-shot images. *arXiv:2311.13398*, 2023a.
- Wang Yifan, Felice Serena, Shihao Wu, Cengiz Öztireli, and Olga Sorkine-Hornung. Differentiable surface splatting for point-based geometry processing. *ACM TOG*, 38(6):1–14, 2019.
- Jonathan T Barron, Ben Mildenhall, Dor Verbin, Pratul P Srinivasan, and Peter Hedman. Mip-nerf 360: Unbounded anti-aliased neural radiance fields. In *CVPR*, pages 5470–5479, 2022.
- Arno Knapitsch, Jaesik Park, Qian-Yi Zhou, and Vladlen Koltun. Tanks and temples: Benchmarking large-scale scene reconstruction. *ACM TOG*, 36(4):1–13, 2017.
- Peter Hedman, Julien Philip, True Price, Jan-Michael Frahm, George Drettakis, and Gabriel Brostow. Deep blending for free-viewpoint image-based rendering. *ACM TOG*, 37(6):1–15, 2018.
- Tianye Li, Mira Slavcheva, Michael Zollhoefer, Simon Green, Christoph Lassner, Changil Kim, Tanner Schmidt, Steven Lovegrove, Michael Goesele, Richard Newcombe, et al. Neural 3d video synthesis from multi-view video. In *CVPR*, pages 5521–5531, 2022.
- Albert Pumarola, Enric Corona, Gerard Pons-Moll, and Francesc Moreno-Noguer. D-nerf: Neural radiance fields for dynamic scenes. In *CVPR*, pages 10318–10327, 2021.
- Ben Mildenhall, Pratul P. Srinivasan, Rodrigo Ortiz-Cayon, Nima Khademi Kalantari, Ravi Ramamoorthi, Ren Ng, and Abhishek Kar. Local light field fusion: Practical view synthesis with prescriptive sampling guidelines. *ACM TOG*, 2019.
- Tinghui Zhou, Richard Tucker, John Flynn, Graham Fyffe, and Noah Snavely. Stereo magnification: learning view synthesis using multiplane images. *ACM TOG*, 37(4):1–12, 2018.
- Andrew Liu, Richard Tucker, Varun Jampani, Ameesh Makadia, Noah Snavely, and Angjoo Kanazawa. Infinite nature: Perpetual view generation of natural scenes from a single image. In *ICCV*, pages 14458–14467, 2021.
- Angel X Chang, Thomas Funkhouser, Leonidas Guibas, Pat Hanrahan, Qixing Huang, Zimo Li, Silvio Savarese, Manolis Savva, Shuran Song, Hao Su, et al. Shapenet: An information-rich 3d model repository. *arXiv:1512.03012*, 2015.
- Ruizhi Shao, Zerong Zheng, Hanzhang Tu, Boning Liu, Hongwen Zhang, and Yebin Liu. Tensor4d: Efficient neural 4d decomposition for high-fidelity dynamic reconstruction and rendering. In *CVPR*, pages 16632–16642, 2023a.
- Kacper Kania, Kwang Moo Yi, Marek Kowalski, Tomasz Trzciniński, and Andrea Tagliasacchi. Conerf: Controllable neural radiance fields. In *CVPR*, pages 18623–18632, 2022.

- Gyeongsik Moon, Shoou-I Yu, He Wen, Takaaki Shiratori, and Kyoung Mu Lee. Interhand2.6m: A dataset and baseline for 3d interacting hand pose estimation from a single rgb image. In *ECCV*, pages 548–564. Springer, 2020.
- Zhongzheng Ren, Aseem Agarwala, Bryan Russell, Alexander G Schwing, and Oliver Wang. Neural volumetric object selection. In *CVPR*, pages 6133–6142, 2022.
- Ashkan Mirzaei, Tristan Aumentado-Armstrong, Konstantinos G Derpanis, Jonathan Kelly, Marcus A Brubaker, Igor Gilitschenski, and Alex Levinshtein. Spin-nerf: Multiview segmentation and perceptual inpainting with neural radiance fields. In *CVPR*, pages 20669–20679, 2023.
- Justin Kerr, Chung Min Kim, Ken Goldberg, Angjoo Kanazawa, and Matthew Tancik. Lerf: Language embedded radiance fields. In *CVPR*, pages 19729–19739, 2023.
- Julian Straub, Thomas Whelan, Lingni Ma, Yufan Chen, Erik Wijmans, Simon Green, Jakob J Engel, Raul Mur-Artal, Carl Ren, Shobhit Verma, et al. The replica dataset: A digital replica of indoor spaces. *arXiv:1906.05797*, 2019.
- Andreas Geiger, Philip Lenz, and Raquel Urtasun. Are we ready for autonomous driving? the kitti vision benchmark suite. In *CVPR*, pages 3354–3361. IEEE, 2012.
- Matt Deitke, Dustin Schwenk, Jordi Salvador, Luca Weihs, Oscar Michel, Eli VanderBilt, Ludwig Schmidt, Kiana Ehsani, Aniruddha Kembhavi, and Ali Farhadi. Objaverse: A universe of annotated 3d objects. In *CVPR*, pages 13142–13153, 2023.
- Tong Wu, Jiarui Zhang, Xiao Fu, Yuxin Wang, Jiawei Ren, Liang Pan, Wayne Wu, Lei Yang, Jiaqi Wang, Chen Qian, et al. Omnibject3d: Large-vocabulary 3d object dataset for realistic perception, reconstruction and generation. In *CVPR*, pages 803–814, 2023b.
- Thiemo Alldieck, Marcus Magnor, Weipeng Xu, Christian Theobalt, and Gerard Pons-Moll. Video based reconstruction of 3d people models. In *CVPR*, pages 8387–8397, 2018.
- Marc Habermann, Lingjie Liu, Weipeng Xu, Michael Zollhoefer, Gerard Pons-Moll, and Christian Theobalt. Real-time deep dynamic characters. *ACM TOG*, 40(4):1–16, 2021.
- Sida Peng, Yuanqing Zhang, Yinghao Xu, Qianqian Wang, Qing Shuai, Hujun Bao, and Xiaowei Zhou. Neural body: Implicit neural representations with structured latent codes for novel view synthesis of dynamic humans. In *CVPR*, pages 9054–9063, 2021.
- Zerong Zheng, Han Huang, Tao Yu, Hongwen Zhang, Yandong Guo, and Yebin Liu. Structured local radiance fields for human avatar modeling. In *CVPR*, pages 15893–15903, 2022.
- Wei Jiang, Kwang Moo Yi, Golnoosh Samei, Oncel Tuzel, and Anurag Ranjan. Neuman: Neural human radiance field from a single video. In *ECCV*, pages 402–418. Springer, 2022.
- Mustafa İşik, Martin Rünz, Markos Georgopoulos, Taras Khakhulin, Jonathan Starck, Lourdes Agapito, and Matthias Nießner. Humanrf: High-fidelity neural radiance fields for humans in motion. *arXiv:2305.06356*, 2023.
- Yingwenqi Jiang, Jiadong Tu, Yuan Liu, Xifeng Gao, Xiaoxiao Long, Wenping Wang, and Yuexin Ma. Gaussianshader: 3d gaussian splatting with shading functions for reflective surfaces. *arXiv:2311.17977*, 2023a.
- Agelos Kratimenos, Jiahui Lei, and Kostas Daniilidis. Dynmf: Neural motion factorization for real-time dynamic view synthesis with 3d gaussian splatting. *arXiv:2312.00112*, 2023.
- Zehao Zhu, Zhiwen Fan, Yifan Jiang, and Zhangyang Wang. Fsgs: Real-time few-shot view synthesis using gaussian splatting. *arXiv:2312.00451*, 2023.
- Johannes L Schonberger and Jan-Michael Frahm. Structure-from-motion revisited. In *CVPR*, pages 4104–4113, 2016.
- Stephen Lombardi, Tomas Simon, Gabriel Schwartz, Michael Zollhoefer, Yaser Sheikh, and Jason Saragih. Mixture of volumetric primitives for efficient neural rendering. *ACM TOG*, 40(4):1–13, 2021.
- William H Equitz. A new vector quantization clustering algorithm. *IEEE Transactions on Acoustics, Speech, and Signal Processing*, 37(10):1568–1575, 1989.
- KL Navaneet, Kossar Pourahmadi Meibodi, Soroush Abbasi Koohpayegani, and Hamed Pirsiavash. Compact3d: Compressing gaussian splat radiance field models with vector quantization. *arXiv:2311.18159*, 2023.
- Sharath Girish, Kamal Gupta, and Abhinav Shrivastava. Eagles: Efficient accelerated 3d gaussians with lightweight encodings. *arXiv:2312.04564*, 2023.
- Zhiwen Fan, Kevin Wang, Kairun Wen, Zehao Zhu, Deja Xu, and Zhangyang Wang. Lightgaussian: Unbounded 3d gaussian compression with 15x reduction and 200+ fps. *arXiv:2311.17245*, 2023.
- Kai Katsumata, Duc Minh Vo, and Hideki Nakayama. An efficient 3d gaussian representation for monocular/multi-view dynamic scenes. *arXiv:2311.12897*, 2023.

- Zhiwen Yan, Weng Fei Low, Yu Chen, and Gim Hee Lee. Multi-scale 3d gaussian splatting for anti-aliased rendering. *arXiv:2311.17089*, 2023a.
- Harry Nyquist. Certain topics in telegraph transmission theory. *Transactions of the American Institute of Electrical Engineers*, 47(2):617–644, 1928.
- Claude E Shannon. Communication in the presence of noise. *Proceedings of the IRE*, 37(1):10–21, 1949.
- Ben Mildenhall, Peter Hedman, Ricardo Martin-Brualla, Pratul P Srinivasan, and Jonathan T Barron. Nerf in the dark: High dynamic range view synthesis from noisy raw images. In *CVPR*, pages 16190–16199, 2022.
- Richard Szeliski. *Computer vision: algorithms and applications*. Springer Nature, 2022.
- Jian Gao, Chun Gu, Youtian Lin, Hao Zhu, Xun Cao, Li Zhang, and Yao Yao. Relightable 3d gaussian: Real-time point cloud relighting with brdf decomposition and ray tracing. *arXiv:2311.16043*, 2023.
- Yao Yao, Zixin Luo, Shiwei Li, Tian Fang, and Long Quan. Mvsnet: Depth inference for unstructured multi-view stereo. In *ECCV*, pages 767–783, 2018.
- Yao Yao, Jingyang Zhang, Jingbo Liu, Yihang Qu, Tian Fang, David McKinnon, Yanghai Tsin, and Long Quan. Neif: Neural incident light field for physically-based material estimation. In *ECCV*, pages 700–716. Springer, 2022.
- Tero Karras. Maximizing parallelism in the construction of bvhs, octrees, and k-d trees. In *ACM SIGGRAPH*, pages 33–37, 2012.
- James T Kajiya. The rendering equation. In *Proceedings of the 13th Annual Conference on Computer Graphics and Interactive Techniques*, pages 143–150, 1986.
- Zhihao Liang, Qi Zhang, Ying Feng, Ying Shan, and Kui Jia. Gs-ir: 3d gaussian splatting for inverse rendering. *arXiv:2311.16473*, 2023a.
- Brian Karis and Epic Games. Real shading in unreal engine 4. *Proc. Physically Based Shading Theory Practice*, 4(3):1, 2013.
- Li Ma, Vasu Agrawal, Haithem Turki, Changil Kim, Chen Gao, Pedro Sander, Michael Zollhöfer, and Christian Richardt. Specnerf: Gaussian directional encoding for specular reflections. *arXiv:2312.13102*, 2023.
- Ainaz Eftekhari, Alexander Sax, Jitendra Malik, and Amir Zamir. Omnidata: A scalable pipeline for making multi-task mid-level vision datasets from 3d scans. In *ICCV*, pages 10786–10796, 2021.
- Clément Godard, Oisín Mac Aodha, and Gabriel J Brostow. Unsupervised monocular depth estimation with left-right consistency. In *CVPR*, pages 270–279, 2017.
- John Canny. A computational approach to edge detection. *IEEE TPAMI*, (6):679–698, 1986.
- Denis Zorin, Peter Schröder, and Wim Sweldens. Interpolating subdivision for meshes with arbitrary topology. In *Proceedings of the 23rd Annual Conference on Computer Graphics and Interactive Techniques*, pages 189–192, 1996.
- Haolin Xiong, Sairisheek Muttukuru, Rishi Upadhyay, Pradyumna Chari, and Achuta Kadambi. Sparsegs: Real-time 360 $\{\deg\}$ sparse view synthesis using gaussian splatting. *arXiv:2312.00206*, 2023.
- Xiaoxiao Long, Cheng Lin, Peng Wang, Taku Komura, and Wenping Wang. Sparseneus: Fast generalizable neural surface reconstruction from sparse views. In *ECCV*, pages 210–227. Springer, 2022.
- Katrin Lasinger, René Ranftl, Konrad Schindler, and Vladlen Koltun. Towards robust monocular depth estimation: Mixing datasets for zero-shot cross-dataset transfer. *arXiv:1907.01341*, 2019.
- S Mahdi H Miangoleh, Sebastian Dille, Long Mai, Sylvain Paris, and Yagiz Aksoy. Boosting monocular depth estimation models to high-resolution via content-adaptive multi-resolution merging. In *CVPR*, pages 9685–9694, 2021.
- Ben Poole, Ajay Jain, Jonathan T Barron, and Ben Mildenhall. Dreamfusion: Text-to-3d using 2d diffusion. *arXiv:2209.14988*, 2022.
- Sara Fridovich-Keil, Giacomo Meanti, Frederik Rahbæk Warburg, Benjamin Recht, and Angjoo Kanazawa. K-planes: Explicit radiance fields in space, time, and appearance. In *CVPR*, pages 12479–12488, 2023.
- Bardienus P Duisterhof, Zhao Mandi, Yunchao Yao, Jia-Wei Liu, Mike Zheng Shou, Shuran Song, and Jeffrey Ichnowski. Md-splatting: Learning metric deformation from 4d gaussians in highly deformable scenes. *arXiv:2312.00583*, 2023.
- Ang Cao and Justin Johnson. Hexplane: A fast representation for dynamic scenes. In *CVPR*, pages 130–141, 2023.
- Jonathon Luiten, Georgios Kopanas, Bastian Leibe, and Deva Ramanan. Dynamic 3d gaussians: Tracking by persistent dynamic view synthesis. *arXiv:2308.09713*, 2023.

- Zeyu Yang, Hongye Yang, Zijie Pan, Xiatian Zhu, and Li Zhang. Real-time photorealistic dynamic scene representation and rendering with 4d gaussian splatting. *arXiv:2310.10642*, 2023a.
- Tianyi Xie, Zeshun Zong, Yuxin Qiu, Xuan Li, Yutao Feng, Yin Yang, and Chenfanfu Jiang. Physgaussian: Physics-integrated 3d gaussians for generative dynamics. *arXiv:2311.12198*, 2023.
- Stanislaw Szymanowicz, Christian Rupprecht, and Andrea Vedaldi. Splatter image: Ultra-fast single-view 3d reconstruction. *arXiv:2312.13150*, 2023.
- Zheheng Jiang, Hossein Rahmani, Sue Black, and Bryan M Williams. 3d points splatting for real-time dynamic hand reconstruction. *arXiv:2312.13770*, 2023b.
- Hanlin Chen, Chen Li, and Gim Hee Lee. Neusg: Neural implicit surface reconstruction with 3d gaussian splatting guidance. *arXiv:2312.00846*, 2023a.
- Peng Wang, Lingjie Liu, Yuan Liu, Christian Theobalt, Taku Komura, and Wenping Wang. Neus: Learning neural implicit surfaces by volume rendering for multi-view reconstruction. In *NIPS*, pages 27171–27183. Curran Associates, Inc., 2021.
- David Charatan, Sizhe Li, Andrea Tagliasacchi, and Vincent Sitzmann. pixelsplat: 3d gaussian splats from image pairs for scalable generalizable 3d reconstruction. *arXiv:2312.12337*, 2023.
- Zi-Xin Zou, Zhipeng Yu, Yuan-Chen Guo, Yangguang Li, Ding Liang, Yan-Pei Cao, and Song-Hai Zhang. Triplane meets gaussian splatting: Fast and generalizable single-view 3d reconstruction with transformers. *arXiv:2312.09147*, 2023.
- Devikalyan Das, Christopher Wewer, Raza Yunus, Eddy Ilg, and Jan Eric Lenssen. Neural parametric gaussians for monocular non-rigid object reconstruction. *arXiv:2312.01196*, 2023.
- Youtian Lin, Zuozhuo Dai, Siyu Zhu, and Yao Yao. Gaussian-flow: 4d reconstruction with dynamic 3d gaussian particle. *arXiv:2312.03431*, 2023.
- Ziyi Yang, Xinyu Gao, Wen Zhou, Shaohui Jiao, Yuqing Zhang, and Xiaogang Jin. Deformable 3d gaussians for high-fidelity monocular dynamic scene reconstruction. *arXiv:2309.13101*, 2023b.
- Yurui Chen, Chun Gu, Junzhe Jiang, Xiatian Zhu, and Li Zhang. Periodic vibration gaussian: Dynamic urban scene reconstruction and real-time rendering. *arXiv:2311.18561*, 2023b.
- Yi-Hua Huang, Yang-Tian Sun, Ziyi Yang, Xiaoyang Lyu, Yan-Pei Cao, and Xiaojuan Qi. Sc-gs: Sparse-controlled gaussian splatting for editable dynamic scenes. *arXiv:2312.14937*, 2023a.
- Zehranaz Canfes, M Furkan Atasoy, Alara Dirik, and Pinar Yanardag. Text and image guided 3d avatar generation and manipulation. In *WACV*, pages 4421–4431, 2023.
- Cuican Yu, Guansong Lu, Yihan Zeng, Jian Sun, Xiaodan Liang, Huibin Li, Zongben Xu, Songcen Xu, Wei Zhang, and Hang Xu. Towards high-fidelity text-guided 3d face generation and manipulation using only images. In *ICCV*, pages 15326–15337, 2023b.
- Sungwon Hwang, Junha Hyung, Daejin Kim, Min-Jung Kim, and Jaegul Choo. Faceclipnerf: Text-driven 3d face manipulation using deformable neural radiance fields. In *ICCV*, pages 3469–3479, 2023.
- Jiemin Fang, Junjie Wang, Xiaopeng Zhang, Lingxi Xie, and Qi Tian. Gaussianeditor: Editing 3d gaussians delicately with text instructions. *arXiv:2311.16037*, 2023.
- Edgar Tretschk, Ayush Tewari, Vladislav Golyanik, Michael Zollhöfer, Christoph Lassner, and Christian Theobalt. Non-rigid neural radiance fields: Reconstruction and novel view synthesis of a dynamic scene from monocular video. In *ICCV*, pages 12959–12970, 2021.
- Verica Lazova, Vladimir Guzov, Kyle Olszewski, Sergey Tulyakov, and Gerard Pons-Moll. Control-nerf: Editable feature volumes for scene rendering and manipulation. In *WACV*, pages 4340–4350, 2023.
- Tianhan Xu and Tatsuya Harada. Deforming radiance fields with cages. In *ECCV*, pages 159–175. Springer, 2022.
- Chandradeep Pokhariya, Ishaan N Shah, Angela Xing, Zekun Li, Kefan Chen, Avinash Sharma, and Srinath Sridhar. Manus: Markerless hand-object grasp capture using articulated 3d gaussians. *arXiv:2312.02137*, 2023.
- Jiahui Lei, Yufu Wang, Georgios Pavlakos, Lingjie Liu, and Kostas Daniilidis. Gart: Gaussian articulated template models. *arXiv:2311.16099*, 2023.
- Lin Gao, Jie Yang, Bo-Tao Zhang, Jia-Mu Sun, Yu-Jie Yuan, Hongbo Fu, and Yu-Kun Lai. Mesh-based gaussian splatting for real-time large-scale deformation. *arXiv:2402.04796*, 2024.
- Jiajun Huang and Hongchuan Yu. Point’n move: Interactive scene object manipulation on gaussian splatting radiance fields. *arXiv:2311.16737*, 2023.

- Yiwen Chen, Zilong Chen, Chi Zhang, Feng Wang, Xiaofeng Yang, Yikai Wang, Zhongang Cai, Lei Yang, Huaping Liu, and Guosheng Lin. Gaussianeditor: Swift and controllable 3d editing with gaussian splatting. *arXiv:2311.14521*, 2023c.
- Ruizhi Shao, Jingxiang Sun, Cheng Peng, Zerong Zheng, Boyao Zhou, Hongwen Zhang, and Yebin Liu. Control4d: Dynamic portrait editing by learning 4d gan from 2d diffusion-based editor. *arXiv:2305.20082*, 2023b.
- Heng Yu, Joel Julin, Zoltán Á Milacski, Koichiro Niinuma, and László A Jeni. Cogs: Controllable gaussian splatting. *arXiv:2312.05664*, 2023c.
- Jiaxiang Tang, Jiawei Ren, Hang Zhou, Ziwei Liu, and Gang Zeng. Dreamgaussian: Generative gaussian splatting for efficient 3d content creation. *arXiv:2309.16653*, 2023.
- Hao Ouyang, Kathryn Heal, Stephen Lombardi, and Tiancheng Sun. Text2immersion: Generative immersive scene with 3d gaussians. *arXiv:2312.09242*, 2023.
- Linqi Zhou, Andy Shih, Chenlin Meng, and Stefano Ermon. Dreampropeller: Supercharge text-to-3d generation with parallel sampling. *arXiv:2311.17082*, 2023a.
- Yuyang Yin, Dejjia Xu, Zhangyang Wang, Yao Zhao, and Yunchao Wei. 4dgen: Grounded 4d content generation with spatial-temporal consistency. *arXiv:2312.17225*, 2023.
- Taoran Yi, Jiemin Fang, Guanjun Wu, Lingxi Xie, Xiaopeng Zhang, Wenyu Liu, Qi Tian, and Xinggang Wang. Gaussiandreamer: Fast generation from text to 3d gaussian splatting with point cloud priors. *arXiv:2310.08529*, 2023.
- Zilong Chen, Feng Wang, and Huaping Liu. Text-to-3d using gaussian splatting. *arXiv:2309.16585*, 2023d.
- Mohammadreza Armandpour, Huangjie Zheng, Ali Sadeghian, Amir Sadeghian, and Mingyuan Zhou. Re-imagine the negative prompt algorithm: Transform 2d diffusion into 3d, alleviate janus problem and beyond. *arXiv:2304.04968*, 2023.
- Alex Nichol, Heewoo Jun, Prafulla Dhariwal, Pamela Mishkin, and Mark Chen. Point-e: A system for generating 3d point clouds from complex prompts. *arXiv:2212.08751*, 2022.
- Dejjia Xu, Ye Yuan, Morteza Mardani, Sifei Liu, Jiaming Song, Zhangyang Wang, and Arash Vahdat. Agg: Amortized generative 3d gaussians for single image to 3d. *arXiv:2401.04099*, 2024.
- Yixun Liang, Xin Yang, Jiantao Lin, Haodong Li, Xiaogang Xu, and Yingcong Chen. Luciddreamer: Towards high-fidelity text-to-3d generation via interval score matching. *arXiv:2311.11284*, 2023b.
- Alexander Vilesov, Pradyumna Chari, and Achuta Kadambi. Cg3d: Compositional generation for text-to-3d via gaussian splatting. *arXiv:2311.17907*, 2023.
- Jaeyoung Chung, Suyoung Lee, Hyeongjin Nam, Jaerin Lee, and Kyoung Mu Lee. Luciddreamer: Domain-free generation of 3d gaussian splatting scenes. *arXiv:2311.13384*, 2023b.
- Robin Rombach, Andreas Blattmann, Dominik Lorenz, Patrick Esser, and Björn Ommer. High-resolution image synthesis with latent diffusion models. In *CVPR*, pages 10684–10695, 2022.
- Monther Alfuraidan and Qamrul Ansari. *Fixed point theory and graph theory: Foundations and integrative approaches*. Academic Press, 2016.
- Huan Ling, Seung Wook Kim, Antonio Torralba, Sanja Fidler, and Karsten Kreis. Align your gaussians: Text-to-4d with dynamic 3d gaussians and composed diffusion models. *arXiv:2312.13763*, 2023.
- Yuan Liu, Cheng Lin, Zijiao Zeng, Xiaoxiao Long, Lingjie Liu, Taku Komura, and Wenping Wang. Syncdreamer: Generating multiview-consistent images from a single-view image. *arXiv:2309.03453*, 2023a.
- Jiawei Ren, Liang Pan, Jiaxiang Tang, Chi Zhang, Ang Cao, Gang Zeng, and Ziwei Liu. Dreamgaussian4d: Generative 4d gaussian splatting. *arXiv:2312.17142*, 2023.
- Zijie Pan, Zeyu Yang, Xiatian Zhu, and Li Zhang. Fast dynamic 3d object generation from a single-view video. *arXiv:2401.08742*, 2024.
- Shijie Zhou, Haoran Chang, Sicheng Jiang, Zhiwen Fan, Zehao Zhu, Dejjia Xu, Pradyumna Chari, Suya You, Zhangyang Wang, and Achuta Kadambi. Feature 3dgs: Supercharging 3d gaussian splatting to enable distilled feature fields. *arXiv:2312.03203*, 2023b.
- Jin-Chuan Shi, Miao Wang, Hao-Bin Duan, and Shao-Hua Guan. Language embedded 3d gaussians for open-vocabulary scene understanding. *arXiv:2311.18482*, 2023.
- Mingqiao Ye, Martin Danelljan, Fisher Yu, and Lei Ke. Gaussian grouping: Segment and edit anything in 3d scenes. *arXiv:2312.00732*, 2023.

- Yunzhi Yan, Haotong Lin, Chenxu Zhou, Weijie Wang, Haiyang Sun, Kun Zhan, Xianpeng Lang, Xiaowei Zhou, and Sida Peng. Street gaussians for modeling dynamic urban scenes. *arXiv:2401.01339*, 2024.
- Xingxing Zuo, Pouya Samangouei, Yunwen Zhou, Yan Di, and Mingyang Li. Fmgs: Foundation model embedded 3d gaussian splatting for holistic 3d scene understanding. *arXiv:2401.01970*, 2024.
- Kun Lan, Haoran Li, Haolin Shi, Wenjun Wu, Yong Liao, Lin Wang, and Pengyuan Zhou. 2d-guided 3d gaussian segmentation. *arXiv:2312.16047*, 2023.
- Alexander Kirillov, Eric Mintun, Nikhila Ravi, Hanzi Mao, Chloe Rolland, Laura Gustafson, Tete Xiao, Spencer Whitehead, Alexander C Berg, Wan-Yen Lo, et al. Segment anything. *arXiv:2304.02643*, 2023.
- Youquan Liu, Lingdong Kong, Jun Cen, Runnan Chen, Wenwei Zhang, Liang Pan, Kai Chen, and Ziwei Liu. Segment any point cloud sequences by distilling vision foundation models. *arXiv:2306.09347*, 2023b.
- Jiazhong Cen, Jiemin Fang, Chen Yang, Lingxi Xie, Xiaopeng Zhang, Wei Shen, and Qi Tian. Segment any 3d gaussians. *arXiv:2312.00860*, 2023.
- Xu Hu, Yuxi Wang, Lue Fan, Junsong Fan, Junran Peng, Zhen Lei, Qing Li, and Zhaoxiang Zhang. Semantic anything in 3d gaussians. *arXiv:2401.17857*, 2024.
- Xiaoyu Zhou, Zhiwei Lin, Xiaojun Shan, Yongtao Wang, Deqing Sun, and Ming-Hsuan Yang. Drivingsgussian: Composite gaussian splatting for surrounding dynamic autonomous driving scenes. *arXiv:2312.07920*, 2023c.
- Chi Yan, Delin Qu, Dong Wang, Dan Xu, Zhigang Wang, Bin Zhao, and Xuelong Li. Gs-slam: Dense visual slam with 3d gaussian splatting. *arXiv:2311.11700*, 2023b.
- Hidenobu Matsuki, Riku Murai, Paul HJ Kelly, and Andrew J Davison. Gaussian splatting slam. *arXiv:2312.06741*, 2023.
- Huajian Huang, Longwei Li, Hui Cheng, and Sai-Kit Yeung. Photo-slam: Real-time simultaneous localization and photorealistic mapping for monocular, stereo, and rgb-d cameras. *arXiv:2311.16728*, 2023b.
- Nikhil Keetha, Jay Karhade, Krishna Murthy Jatavallabhula, Gengshan Yang, Sebastian Scherer, Deva Ramanan, and Jonathon Luiten. Splatam: Splat, track & map 3d gaussians for dense rgb-d slam. *arXiv:2312.02126*, 2023.
- Vladimir Yugay, Yue Li, Theo Gevers, and Martin R Oswald. Gaussian-slam: Photo-realistic dense slam with gaussian splatting. *arXiv:2312.10070*, 2023.
- Yuan Sun, Xuan Wang, Yunfan Zhang, Jie Zhang, Caigui Jiang, Yu Guo, and Fei Wang. icomma: Inverting 3d gaussians splatting for camera pose estimation via comparing and matching. *arXiv:2312.09031*, 2023.
- Rohit Jena, Ganesh Subramanian Iyer, Siddharth Choudhary, Brandon Smith, Pratik Chaudhari, and James Gee. Splatarmor: Articulated gaussian splatting for animatable humans from monocular rgb videos. *arXiv:2311.10812*, 2023.
- Arthur Moreau, Jifei Song, Helisa Dharmo, Richard Shaw, Yiren Zhou, and Eduardo Pérez-Pellitero. Human gaussian splatting: Real-time rendering of animatable avatars. *arXiv:2311.17113*, 2023.
- Mengtian Li, Shengxiang Yao, Zhifeng Xie, Keyu Chen, and Yu-Gang Jiang. Gaussianbody: Clothed human reconstruction via 3d gaussian splatting. *arXiv:2401.09720*, 2024.
- Shenhan Qian, Tobias Kirschstein, Liam Schoneveld, Davide Davoli, Simon Giebenhain, and Matthias Nießner. Gaussianavatars: Photorealistic head avatars with rigged 3d gaussians. *arXiv:2312.02069*, 2023a.
- Zhe Li, Zerong Zheng, Lizhen Wang, and Yebin Liu. Animatable gaussians: Learning pose-dependent gaussian maps for high-fidelity human avatar modeling. *arXiv:2311.16096*, 2023a.
- Lizhen Wang, Xiaochen Zhao, Jingxiang Sun, Yuxiang Zhang, Hongwen Zhang, Tao Yu, and Yebin Liu. Styleavatar: Real-time photo-realistic portrait avatar from a single video. *arXiv:2305.00942*, 2023a.
- Haokai Pang, Heming Zhu, Adam Kortylewski, Christian Theobalt, and Marc Habermann. Ash: Animatable gaussian splats for efficient and photoreal human rendering. *arXiv:2312.05941*, 2023.
- Ladislav Kavan, Steven Collins, Jiří Žára, and Carol O’Sullivan. Skinning with dual quaternions. In *Proceedings of the 2007 Symposium on Interactive 3D Graphics and Games*, pages 39–46, 2007.
- Wojciech Zielonka, Timur Bagautdinov, Shunsuke Saito, Michael Zollhöfer, Justus Thies, and Javier Romero. Drivable 3d gaussian avatars. *arXiv:2311.08581*, 2023.
- Yuheng Jiang, Zhehao Shen, Penghao Wang, Zhuo Su, Yu Hong, Yingliang Zhang, Jingyi Yu, and Lan Xu. Hifi4g: High-fidelity human performance rendering via compact gaussian splatting. *arXiv:2312.03461*, 2023c.
- Yiming Wang, Qin Han, Marc Habermann, Kostas Daniilidis, Christian Theobalt, and Lingjie Liu. Neus2: Fast learning of neural implicit surfaces for multi-view reconstruction. In *CVPR*, pages 3295–3306, 2023b.

- Robert W Sumner, Johannes Schmid, and Mark Pauly. Embedded deformation for shape manipulation. In *ACM SIGGRAPH*, pages 80–es. 2007.
- Muhammed Kocabas, Jen-Hao Rick Chang, James Gabriel, Oncel Tuzel, and Anurag Ranjan. Hugs: Human gaussian splats. *arXiv:2311.17910*, 2023.
- HyunJun Jung, Nikolas Brasch, Jifei Song, Eduardo Perez-Pellitero, Yiren Zhou, Zhihao Li, Nassir Navab, and Benjamin Busam. Deformable 3d gaussian splatting for animatable human avatars. *arXiv:2312.15059*, 2023.
- Mingwei Li, Jiachen Tao, Zongxin Yang, and Yi Yang. Human101: Training 100+ fps human gaussians in 100s from 1 view. *arXiv:2312.15258*, 2023b.
- Zhiyin Qian, Shaofei Wang, Marko Mihajlovic, Andreas Geiger, and Siyu Tang. 3dgs-avatar: Animatable avatars via deformable 3d gaussian splatting. *arXiv:2312.09228*, 2023b.
- Chung-Yi Weng, Brian Curless, Pratul P Srinivasan, Jonathan T Barron, and Ira Kemelmacher-Shlizerman. Humannerf: Free-viewpoint rendering of moving people from monocular video. In *CVPR*, pages 16210–16220, 2022.
- Liangxiao Hu, Hongwen Zhang, Yuxiang Zhang, Boyao Zhou, Boning Liu, Shengping Zhang, and Liqiang Nie. Gaussianavatar: Towards realistic human avatar modeling from a single video via animatable 3d gaussians. *arXiv:2312.02134*, 2023.
- Shoukang Hu and Ziwei Liu. Gauhuman: Articulated gaussian splatting from monocular human videos. *arXiv:2312.02973*, 2023.
- Tianye Li, Timo Bolkart, Michael J Black, Hao Li, and Javier Romero. Learning a model of facial shape and expression from 4d scans. *ACM TOG*, 36(6):194–1, 2017.
- Helisa Dharmo, Yinyu Nie, Arthur Moreau, Jifei Song, Richard Shaw, Yiren Zhou, and Eduardo Pérez-Pellitero. Headgas: Real-time animatable head avatars via 3d gaussian splatting. *arXiv:2312.02902*, 2023.
- Zhongyuan Zhao, Zhenyu Bao, Qing Li, Guoping Qiu, and Kanglin Liu. Psavatar: A point-based morphable shape model for real-time head avatar creation with 3d gaussian splatting. *arXiv:2401.12900*, 2024.
- Yufan Chen, Lizhen Wang, Qijing Li, Hongjiang Xiao, Shengping Zhang, Hongxun Yao, and Yebin Liu. Monogaussianavatar: Monocular gaussian point-based head avatar. *arXiv:2312.04558*, 2023e.
- Yuelang Xu, Benwang Chen, Zhe Li, Hongwen Zhang, Lizhen Wang, Zerong Zheng, and Yebin Liu. Gaussian head avatar: Ultra high-fidelity head avatar via dynamic gaussians. *arXiv:2312.03029*, 2023a.
- Jie Wang, Jiu-Cheng Xie, Xianyan Li, Feng Xu, Chi-Man Pun, and Hao Gao. Gaussianhead: Impressive head avatars with learnable gaussian diffusion. *arXiv:2312.01632*, 2023c.
- Shunyuang Zheng, Boyao Zhou, Ruizhi Shao, Boning Liu, Shengping Zhang, Liqiang Nie, and Yebin Liu. Gps-gaussian: Generalizable pixel-wise 3d gaussian splatting for real-time human novel view synthesis. *arXiv:2312.02155*, 2023.
- Linning Xu, Yuanbo Xiangli, Sida Peng, Xingang Pan, Nanxuan Zhao, Christian Theobalt, Bo Dai, and Dahua Lin. Grid-guided neural radiance fields for large urban scenes. In *CVPR*, pages 8296–8306, 2023b.
- Xuan Li, Yi-Ling Qiao, Peter Yichen Chen, Krishna Murthy Jatavallabhula, Ming Lin, Chenfanfu Jiang, and Chuang Gan. Pac-nerf: Physics augmented continuum neural radiance fields for geometry-agnostic system identification. *arXiv:2303.05512*, 2023c.
- Mengyu Chu, Lingjie Liu, Quan Zheng, Erik Franz, Hans-Peter Seidel, Christian Theobalt, and Rhaleb Zayer. Physics informed neural fields for smoke reconstruction with sparse data. *ACM TOG*, 41(4):1–14, 2022.
- Daniel Rebain, Ke Li, Vincent Sitzmann, Soroosh Yazdani, Kwang Moo Yi, and Andrea Tagliasacchi. Deep medial fields. *arXiv:2106.03804*, 2021.
- Yuxin Liu, Minshan Xie, Hanyuan Liu, and Tien-Tsin Wong. Text-guided texturing by synchronized multi-view diffusion. *arXiv:2311.12891*, 2023c.
- Tianshi Cao, Karsten Kreis, Sanja Fidler, Nicholas Sharp, and Kangxue Yin. Textfusion: Synthesizing 3d textures with text-guided image diffusion models. In *ICCV*, pages 4169–4181, 2023.
- Yinghao Xu, Hao Tan, Fujun Luan, Sai Bi, Peng Wang, Jiahao Li, Zifan Shi, Kalyan Sunkavalli, Gordon Wetzstein, Zexiang Xu, et al. Dmv3d: Denoising multi-view diffusion using 3d large reconstruction model. *arXiv:2311.09217*, 2023c.